The Pennsylvania State University
The Graduate School
John and Willie Leone Family Department of Energy and Mineral Engineering

A ROBUST LINEAR-PRESSURE ANALOG FOR THE ANALYSIS OF NATURAL GAS TRANSPORTATION NETWORKS

A Thesis in
Energy and Mineral Engineering
by
Chew Yeong Leong

Submitted in Partial Fulfillment
of the Requirements
for the Degree of

Master of Science
May 2012

The thesis of Chew Yeong Leong was reviewed and approved* by the following:

Luis F. Ayala H.
Associate Professor of Petroleum and Natural Gas Engineering
Thesis Advisor

Michael Adewumi
Vice Provost for Global Programs
Professor of Petroleum and Natural Gas Engineering

R. Larry Grayson
Professor of Energy and Mineral Engineering;
George H., Jr., and Anne B. Deike Chair in Mining Engineering;
Graduate Program Officer of Energy and Mineral Engineering;
Undergraduate Program Officer of Mining Engineering

*Signatures are on file in the Graduate School

ABSTRACT

Reliable analysis of transportation networks is crucial for design and planning purposes. A pipeline network system could range from a simple to very sophisticated and complex arrangement: from a single pipe transporting fluid from a place to another or elaborated as an interconnected set of fluid networks for intra-state or international transportation. As the complexity of the network system grows, the solution for the network model complicates further. For a natural gas network system, the resulting set of fluid flow governing equations is highly non-linear. In such situations, the customary method employed for the solution of a set of non-linear equations is the multivariable Newton-Raphson method despite its potentially negative drawbacks. Newton-Raphson solution protocols demand a good initialization (i.e., a good initial "guess" of the actual solution) for satisfactory performance because convergence is only guaranteed to occur within a potentially narrow neighborhood around the solution vector. This prerequisite can become fairly restrictive for the solution of large gas network systems, where estimations of "good" initial gas load and nodal values across the domain can defy intuition. In addition, some Newton-Raphson formulations require pre-defining flow loops within a network system prior to attempting a solution, which proves to be a challenging task in an extensive network. An alternate, simple yet elegant method to address the aforementioned problems is proposed. The proposed solution methodology retains most advantages of the Newton-nodal method while removing the need for initial guesses and eliminating the need for expensive Jacobian formulations and associated derivative calculations. The resulting linear-pressure analog model is robust, reliable and its

execution and convergence is independent of user-defined initial guesses for nodal pressures and flow rates. This allows the simulation study of a steady-state gas network system to be efficiently and straight-forwardly conducted.

Table of Contents

LIST OF FIGURES

LIST OF TABLES

LIST OF SYMBOLS

Nomenclature

A	pipe cross sectional area [L^2]
B	number of pipe branches in a pipe network [-]
C_{ij}	pipe conductivity for the generalized gas flow equation [$L^4 m^{-1} t$]
C_R	reservoir rock and fluid properties conductivity [$L^4 m^{-1} t$]
C_w	well conductivity [$L^4 m^{-1} t$]
D	fluid demand at a node in a pipe network [$L^3 t^{-1}$]
d	pipe internal diameter [L]
e	pipe roughness [L]
f_F	Fanning friction factor [-]
F_D	AGA drag factors [-]
g	acceleration of gravity [$L t^{-2}$]
g_c	mass/force unit conversion constant [$m L F^{-1} t^{-2}$ where $F = m L t^{-2}$]
	(32.174 lbm ft $lbf^{-1} s^{-2}$ in Imperial units; 1 Kg m $N^{-1} s^{-2}$ in SI)
H	elevation with respect to datum [L]
HP	horsepower [HP]
K	network characteristic matrix
k	iteration number
k_c	compressor constant
L	pipe length [L]
L_e	pipe equivalent length [L]

L_{ij}	linear-analog pipe conductivity [$L^4\ m^{-1}\ t$]
LP	number of independent loops in a pipe network [-]
MW	molecular mass [$m\ n^{-1}$]
M	mass flow rate [$m\ t^{-1}$]
m	diameter exponent [-]
N	number of nodes in a pipe network [-]
n	flow exponent [-]
n_p	polytropic exponent [-]
n_{st}	number of compression stages [-]
O_i	summation of off-diagonal entries in the i-th row for the linear analog method [$L^4\ m^{-1}\ t$]
p	pressure [$m\ L^{-1}\ t^{-2}$ or $F\ L^{-2}$ where $F = m\ L\ t^{-2}$]
P	network pressure vector
q_{Gij}	gas flow rate at standard conditions for pipe (i,j) [$L^3\ t^{-1}$]
R	universal gas constant [$m\ L^2\ T^{-1}\ t^{-2}\ n^{-1}$] (10.7315 psia-ft^3 $lbmol^{-1}\ R^{-1}$ in English units or 8.314 m^3 Pa K^{-1} $gmol^{-1}$]
Re	Reynolds Number [-]
r	pressure ratio for the linear-pressure analog method [-]
r_c	compression ratio [-]
r_w	well pressure compression ratio [-]
S	network supply/consumption vector
SG	fluid specific gravity [-]

s, s_{ij}	pipe elevation parameter [-]
T	absolute temperature [T]
T_{ij}	analog conductivity transform [-]
T_w	analog well conductivity transform [$(m\ L^{-1}\ t^{-2})^{2n-1}$]
v	fluid velocity [$L\ t^{-1}$]
V	volume [L^3]
x	pipe axial axis [L]
Z	fluid compressibility factor [-]
z	pipe elevation axis; or axial component [L]

Greek

η	compressor adiabatic (isentropic) efficiency
ρ	density [lb/ft3]
Δ	delta
β	elevation-dependent integration term in the energy balance [$L\ t^{-2}$]
ρ	fluid density [$m\ L^{-3}$]
μ	fluid dynamic viscosity [$m\ L^{-1}\ t^{-1}$]
φ	gas density dependency on pressure [$t^2\ L^{-2}$]
π	ratio of the circumference of a circle to its diameter = 3.14159265… [-]
γ	ratio of specific heats of gas
$\kappa_W, \kappa_{PA}, \kappa_{PB}$	unit-dependent constants for the gas friction factor equations;
σ_G	unit-dependent constant for the generalized gas flow equation [$T\ t^2\ L^{-2}$]
α	rate-dependent integration term in the energy balance [$m^2\ L^{-5}\ t^{-2}$]

ω	positive integer multiplier (1,2,3…)
ε	tolerance factor

Subscripts

a	acceleration
av	average
c	compressor
e	elevation
f	friction
G	gas
i	pipe entrance
j	pipe exit
p	polytropic
R	reservoir
shut	shut-in
sc	standard conditions (60 F or 520 R and 14.696 psi in English units; 288.71 K and 101.325 KPa in SI)
w, wh	well

ACKNOWLEDGEMENTS

First of all, I would like to express my deepest gratitude to my thesis advisor, Dr. Luis F. Ayala H.. His words of wisdom and expectations on me have always been my strongest fuel for passion and determination to succeed. Without his encouragement, guidance and support, I would never be able to accomplish what I have accomplished today.

I would not be where I am today without the love and caring from my family and friends from Malaysia. To my Dad, Ee Kuan who has always been the one behind my back, giving me the support and opportunity to learn and grow in a congenial environment. To my Mum, Yok June for her endless love, endowing me with blessings and kindness.

I like to take this opportunity to extend my sincere appreciation for Dr. Larry Grayson and Dr. Michael Adewumi for their interest in serving as committee members. I am also indebted to the Dr. Zuleima Karpyn, Dr. Turgay Ertekin, Dr. Li Li, Dr. John Yilin Wang and Dr. Russell Johns for their invaluable knowledge and supervision on my learning experience and professional development in Pennsylvania State University.

Special thanks are given to Muhamad Hadi Zakaria who has been inspirational to me during our friendship in Pennsylvania State University. I also wish to thank my childhood friend, Andrew Leong for being with me during my ups and downs.

CHAPTER 1

INTRODUCTION

Gas transportation and distribution networks around the world involve a remarkable set of highly integrated pipe networks which operate over a wide range of pressures. The ever-increasing demand for gas makes it vital to adapt and expand these systems while at the same time ensuring safe delivery and cost-effective engineering. Model simulation and system analysis play a major role in planning and design stages as they enable engineers to optimize the pipeline networks and decide on the location of non-pipe elements such as compressors (Mohitpour et al., 2007; Menon, 2005). The aim of a static simulation is to estimate the values of pressures at the nodes and flow rates in the pipes (Ayala, 2012; Larock *et al.*, 2000; Kumar, 1987; Osiadacz, 1987).

Most practical situations in fluid transportation involve systems of pipelines that are interconnected forming a network. Natural gas network simulation entails the definition of the mathematical model governing the flow of gas through a transportation and distribution system (Ayala, 2012; Larock *et al.*, 2000; Kumar, 1987; Osiadacz, 1987). Typical networks can be made up of highly integrated pipes in series, pipes in parallel, branching pipes, and looped pipes. Pipeline systems that form an interconnected net or network are composed of two basic elements: nodes and node-connecting elements. Node-connecting elements can include pipe legs, compressor or pumping stations, valves, pressure and flow regulators, among other components. Nodes are the points where two

pipe legs or any other connecting elements intercept or where there is an injection or offtake of fluid. **Figure 1.1** depicts a typical pipeline network schematic, where nodal, supply, and demand locations are highlighted and the type of node-connecting elements is restricted to pipelines.

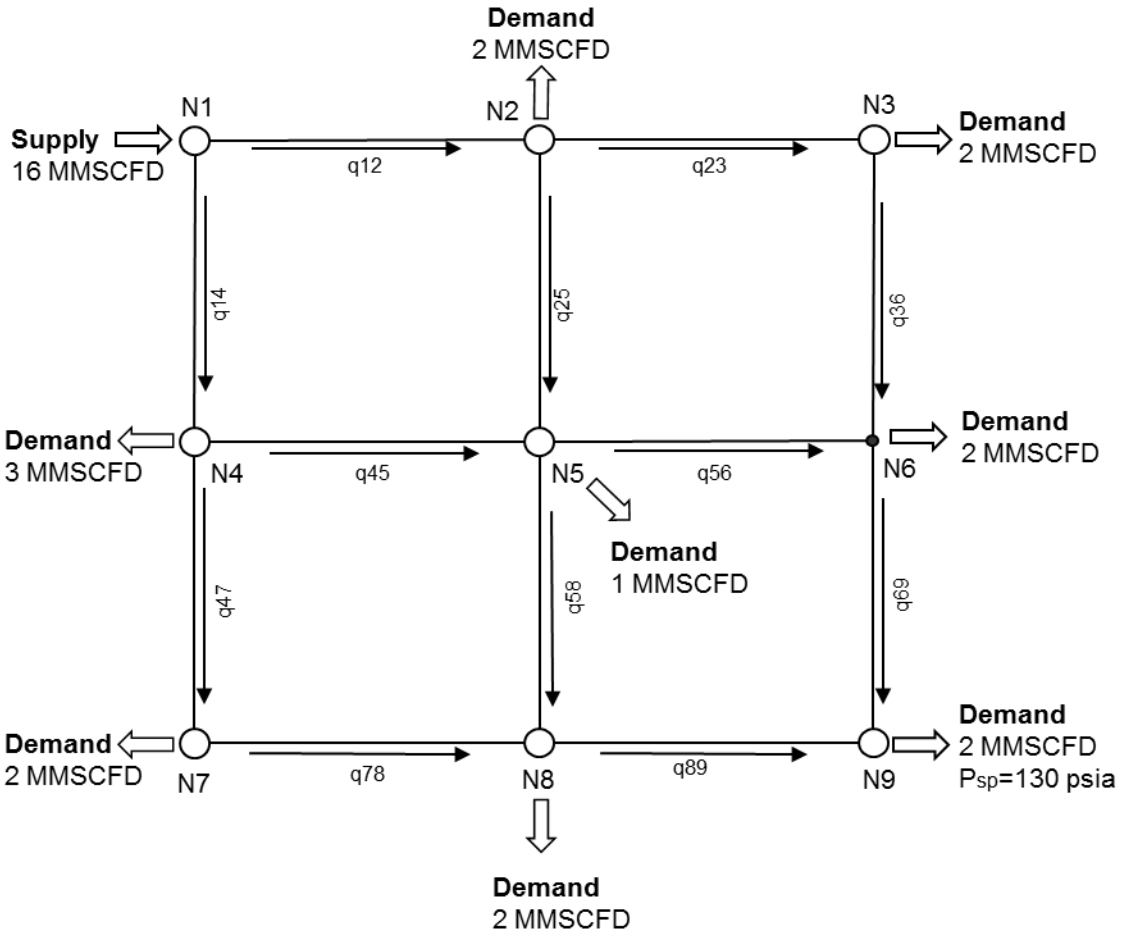

Figure 1.1: A pipeline network schematic

A steady-state network problem can be formulated in a number of ways, but in general, it consists of a system made up of "N" nodes, "B" pipe branches or bridges (edges or arcs),

and “LP” pipe loops as depicted in **Figure 1.1**. It is not uncommon for network systems to have at least one closed-pipe circuit or pipe loop. The presence of pipe loops increases the reliability of delivery of the transported fluid because certain network nodes can be reached simultaneously by more than one pipe. For the gas network in **Figure 1.1**, N=9, B=12, LP=4. Network theory shows that these three quantities are mathematically related through the expression: B = (N-1) + LP, where LP represents the number of independent loops that can be defined in a network graph with N nodes and B branches. In network problems, all physical features of the network are assumed to be known and the analysis consists of determining the resulting flow though each pipe and the associated nodal pressures. This can be accomplished on the basis of known network topology and connectivity information, fluid properties, and pipe characteristics combined with mass and energy conservation statements, as shown in the next sections. This assumes knowledge of the constitutive equation for each node-connecting element—i.e., prior knowledge of the mathematical relationship between flow across the element and its nodal pressures.

A complete natural gas network system usually comprises compressors, wells and several other surface components besides pipelines. A compressor station is one of the most important elements in a natural gas pipeline system. Compressor stations are needed to transport gas in a pipeline. Compressor stations supply the energy to pump gas from production fields to overcome frictional losses in transmission pipelines (Ikoku, 1984). In a long distance pipeline, pipeline pressure by itself is not sufficient to transport the gas

from one location to another. Hence, compressors are installed on the gas pipeline to transport gas from one location to another by providing the additional pressure. For network simulation with a compressor, several important variables associated with the compressor are the flow through the compressor, inlet and outlet pressure, and compression ratio (Osiadacz, 1987). Compression ratio is a cardinal parameter in determining horsepower required to compress a certain volume of gas and also the discharge temperature of gas exiting the compressor. Optimum locations and pressures at which compressor stations operate could then be identified and analyzed through a simulation study. Modeling and understanding the behavior of a network system is not a matter of studying the performance of a single constituent component; but rather one must undertake a comprehensive study of the consequences of the interconnectivity of every component of the system. Traditionally, a gas network system is solved by simplifying the network system with assumptions. In the advent of advanced computer technology, complex designs and heavy computational simulations are no longer time and cost consuming, thus many assumptions are relaxed as numerical simulation proves to be more accessible and sensitivity analysis could be incorporated easily.

Hence, the simultaneous solution of the resulting set of highly non-linear equations enables natural gas network simulation to predict the behavior of highly integrated networks for a number of possible operating conditions. These predictions are routinely used to make design and operational decisions that impact a network system, which take

into account the consequences of interconnectivity and interdependence among all elements within the system.

CHAPTER 2

LITERATURE REVIEW

Fluid pipeline network modeling and development have been traditionally conducted in the area of civil, chemical and mechanical engineering. Throughout the course of history, many empirical approaches had been formulated in order to attempt to capture the different parameters that are believed to be governing the gas flow (Johnson and Berwald, 1935). Most of the equations were formulated based on experimental data and matching field data from operational gas pipeline systems. For example, the Weymouth equation was developed by Thomas R. Weymouth in the 1910s while he was matching compressed air test data flowing through small diameter pipes (Weymouth, 1912). Several decades later, Panhandle-A equation was developed with the intention of proposing flow equations suitable for larger-diameter pipes, since the Weymouth equation overestimated pressure losses for these systems. The "modified" Panhandle-A equation, or Panhandle-B, was then published in 1952 when more empirical data were obtained from the other Panhandle pipelines (Boyd, 1983). Weymouth, Panhandle-A and Panhandle-B equations are popular due to its nature of simplicity and also non-iterative properties. The American Gas Association (AGA) then proposed the AGA equation in the 1960s based on the general gas equation, with a simplified version of Colebrook's friction factor. Ultimately what differs in these equations are the governing friction factor. They could all be expressed in a generalized equation with their own respective friction factor as presented in **Table 3.1** in Chapter 3.

As the need for efficiently utilizing natural gas operations grows, tools capable of handling the resulting problems are also needed. According to Crafton (1976), a steady-state gas pipeline network analysis is a useful design and planning tool as it allows supply and demand optimization, allocation or proration evaluation and compressor optimization. It is, however, vital that the numerical solution procedure of the simulation tool meet two crucial criteria: assurance of rapid solution convergence, uniqueness, thus economical solution costs and also flexibility in handling a wide variety of piping, loop and compressor configurations encountered in gathering and transmission networks.

In a simulation of a natural gas pipeline system, an accurate representation of all components in the pipeline system model is required. In order to minimize the pipeline fuel consumption to maximum extent possible, optimization requires detailed compressor information for each of the individual compressor components (Murphy, 1989). A network problem is eventually expressed in terms of a set of highly non-linear equations for each component in the natural gas network system. It must be solved simultaneously in terms of the desired target unknowns: the ***q***- or nodal-loop formulation has "B" simultaneous equations and the target unknowns are pipe flow rates; the ***p***- or nodal formulation has "N-1" simultaneous equations and solves for nodal pressures; or the $\Delta \boldsymbol{q}$- or loop formulation has "LP" simultaneous equations and solves for loop flows (Ayala, 2012). As the size of network grows, the more complex the resulting system of equations becomes. Throughout the years, a number of protocols for the simplified solution of network equations have been proposed, most notably, the Hardy-Cross method (Cross,

1932) and the Linear Theory method (Wood and Carl, 1972). The Hardy-Cross method, was originally proposed for the analysis of frames in structural engineering by moment distribution, and became widely popular for the analysis of fluid networks because it implemented an iterative scheme readily suitable for hand calculations that circumvented the significant labor of solving the simultaneous set of equations. The Linear Theory method also became a popular approach to approximately linearize the non-linear subset of loop equations within the nodal-loop formulation, but it is also known to suffer from convergence problems.

Osiadacz (1987) then classifies steady-state gas network mathematical methods into Newton-nodal, Newton-loop and Netwon-loop-node, depending on whether they are solving *p*-, Δq-, or *q*- equations, respectively. This classification further emphasizes the widespread use of Newton-Raphson as the method of choice in gas network analysis. Osiadacz (1987) and Li, An and Gedra (2003) discuss the advantages and disadvantages of these three Newton-based methods. The Newton-nodal method is said to be the most straightforward to formulate, creating Jacobian matrixes of large sparsity, but plagued with very poor convergence characteristics due to the well-known initial value problem (i.e., convergence is highly sensitive to starting values) inherent to all locally-convergent Newton-Raphson protocols. Newton-nodal is typically not recommended unless the user has extensive knowledge of the network system and is able to provide very reasonable initial guesses for every nodal pressure. The Newton-loop formulation is based on the application of Kirchoff's second law, which requires the definition of all loops and

knowledge of the spanning tree of the gas network. In this method, a loop flow correction is calculated and applied to all edge flows inside the given loop. The Newton-Raphson procedure is used to drive pressure drops around the loop to zero. This method has better convergence characteristics and is less sensitive to initial guesses. Its major problem is the need for definition of loops, non-unique loops, resulting in a much less sparse Jacobian matrix with sparsity dependent on loop choice. This leads to a more complex solution to formulate than the Newton-nodal method, especially when elements other than pipes are found in the system. In the Newton loop-node method, both loop and nodal equations are used to form a hybrid method of the above two in terms of advantages and disadvantages. All Newton-based methods are still however, prone to lack of convergence and sensitivity to initial guesses, with the nodal formulation being the most susceptible of all. Heavy-reliance on good initial guesses is the staple of every existing method for solving gas network equations—and not only for Newton-based methods but also for the far less-efficient Hardy-Cross and the Linear Theory methods.

Nowadays, the application of the multivariate Newton-Raphson method is rather the norm applied in the simultaneous solution of the large systems of non-linear network equations. However, the most significant limitation of Newton-Raphson methods is their unfortunate tendency of hopelessly diverging when not initialized sufficiently close to the actual solution (i.e., their “local convergence” property). To alleviate this problem, the quadratic local convergence of Newton-Raphson is typically coupled with a globally convergent strategy that can better guarantee progress and convergence towards the

solution (see, for example, Press et al., 2007). However, even for globally-convergent methods, convergence towards a solution is not guaranteed if the initial starting point is too far away from a physically feasible solution. A successful Newton-Raphson implementation thus remains highly dependent on a proper selection of initialization conditions for the problem. In this study, a methodology that remediates this significant shortcoming for gas network modeling is proposed and analyzed.

CHAPTER 3

NETWORK MODEL ANALYSIS

For the purpose of this study, three major components will be identified in a gas network system and analyzed with the proposed methodology: pipeline, compressor and wellheads. Each component in a gas network system could be expressed in a mathematical equation with parameters governed by their respective properties.

In developing the model for single-phase steady-state gas flow in pipeline networks, several assumptions are taken based on engineering judgments or industry's standards (Nagoo, 2003). In the present analysis, it is assumed that:

1) The gas is dry and is considered as a continuum for which basic laws of continuum mechanics still apply.
2) Gas flow is one-dimensional, single-phase and steady-state.
3) Pipelines do not deform regardless of maximum pressure in the pipes.
4) The minimum pressure in a pipe is always above the vapor pressure of gas, hence no liquids are formed.
5) Average gas compressibility and average temperature are assumed to be everywhere in network.
6) Gas is considered to be a Newtonian fluid and polarity effects are negligible.
7) Acceleration effects are negligible.

3.1 Pipe Flow Network Equation

A pipeline is essentially a node-connecting element which connects 2 points together. The interest of the study is the pipeline throughput (flow rate) which depends upon the gas properties, pipe diameter and length, initial gas pressure and temperature, and pressure drop due to friction (Menon, 2005). The following assumptions are used during the development of the generalized gas flow equation in a pipeline for this study:

1) Single-phase one-dimensional flow
2) Steady-state flow along pipe length segment
3) Isothermal flow
4) Constant average gas compressibility
5) Kinetic change along the pipe length segment is negligible
6) Flowing velocity is accurately characterized by apparent bulk average velocity
7) Friction factor is constant along the pipe length segment

The fundamental difference among the specialized formulas for the flow through pipes is how friction factors are evaluated. The most comprehensive approach for the calculation of frictional losses in single-phase compressible fluid flow in pipelines is the application of the General Gas equation where its friction factor is calculated based of Moody's Chart. Section 3.1.1 shows the derivation of the constitutive equation for gas pipe flow from fundamental principles. For the case of single-phase flow of gases in pipes, these constitutive equations are well-known and are presented in **Table 3.1** below.

3.1.1 Derivation of Pipe Flow Equation for Single-Phase Flow

Total pressure losses in pipelines can be calculated as the sum of the contributions of friction losses (i.e., irreversibilities), elevation changes (potential energy differences), and acceleration changes (i.e, kinetic energy differences) as stated below:

$$\left(\frac{dp}{dx}\right)_T = \left(\frac{dp}{dx}\right)_f + \left(\frac{dp}{dx}\right)_e + \left(\frac{dp}{dx}\right)_a \tag{3.1}$$

Equation (3.1) is a restatement of the first law of thermodynamics or modified Bernoulli's equation. Each of the energy terms in this overall energy balance is calculated as follows:

$$\left(\frac{dp}{dx}\right)_f = -\frac{2f\rho v^2}{g_c d} \tag{3.2}$$

$$\left(\frac{dp}{dx}\right)_{elev} = -\rho\frac{g}{g_c}\frac{dz}{dx} \tag{3.3}$$

$$\left(\frac{dp}{dx}\right)_{acc} = -\frac{\rho v}{g_c}\frac{dv}{dx} \tag{3.4}$$

In pipeline flow, the contribution of the kinetic energy term to the overall energy balance is considered insignificant compared to the typical magnitudes of friction losses and potential energy changes. Thus, by integrating this expression from pipe inlet (x=0, p=p_1) to outlet (x=L, p=p_2) and considering $M = \rho vA$ with $A = \pi d^2/4$, one obtains:

$$\int_{p_1}^{p_2} \rho dp = -\alpha\int_0^L dx - \beta\int_0^L \rho^2 dz \tag{3.5}$$

where $\alpha = (32\dot{m}^2 f)/(\pi^2 g_c d^5)$ and $\beta = (g/g_c)(\Delta H/L)$. For the flow of liquids and nearly incompressible fluids, density integrals can be readily resolved and volumetric flow can be shown to be dependent on the difference of linear end pressures. However, for the isothermal flow of gases, the fluid density dependency with pressure ($\rho = \phi p$) introduces a stronger dependency of flow rate on pressure to yield:

$$p_1^2 - e^s p_2^2 = \frac{\alpha}{\eta^2}\frac{(e^s - 1)}{\beta} \tag{3.6}$$

where $\eta = (\gamma_g MW_{air})/(Z_{av} R T_{av})$ and $s = 2\eta\beta L$. Equation (3.6) states the well-known fact that the driving force for gas flow through pipelines is the difference of the squared pressures. Therefore, for inclined pipes, the design equation gas flow in pipelines (evaluated at standard conditions, $W = \rho_{sc} q_{Gsc}$ with $\rho_{sc} = (p_{sc}\gamma_g MW_{air})/(R \cdot T_{sc})$) becomes:

$$q_{Gij} = C_{ij} \cdot (p_i^2 - e^{s_{ij}} p_j^2)^{0.5} \tag{3.7}$$

where "C_{ij}" is the pipe conductivity, $C_{ij} = \left(\frac{\pi^2 g_c R}{64 MW_{air}}\right)^{0.5} \frac{T_{sc}/p_{sc}}{(\gamma_g T_{av} Z_{av})^{0.5}} \frac{d^{2.5}}{f^{0.5} L_e^{0.5}}$, which captures the dependency of friction factor, pipe geometry, and fluid properties on the flow capacity of the pipe. In **Table 3.1**, pipe efficiency, e_f is introduced in the pipe conductivity term as a tuning parameter for calibration purposes to account for any discrepancies in results (Schroeder, 2011). For horizontal flow ($s = \beta = 0$; $(e^s - 1)/\beta \to 1$), this equation becomes:

$$q_{Gij} = C_{ij} \cdot (p_i^2 - p_j^2)^{0.5} \tag{3.8}$$

with $L_e = L$. Depending on the type of friction factor correlation used to evaluate pipe conductivity, Equations (3.7) and (3.8) above can be recast into the different traditional forms of gas pipe flow equations available in the literature such as the equations of Weymouth, Panhandle-A, Panhandle-B, AGA, IGT, and Spitzglass, among others (Ayala, 2012; Mohitpour et al., 2007; Menon, 2005; Kumar, 1987; Osiadacz, 1987).

Table 3.1: Summary of specialized equations for gas flow (adapted from Ayala, 2012)

Generalized Gas Flow Equation: $q_{Gij} = C_{ij} \cdot (p_i^2 - e^s p_j^2)^{0.5}$ with: $C_{ij} = \frac{\sigma_G . e_f}{\sqrt{SG_G T_{av} Z_{av}}} (\frac{T_{sc}}{p_{sc}}) \sqrt{\frac{1}{f_F}} \cdot \frac{d^{2.5}}{L_e^{0.5}}$	
Gas Flow Equation	**Friction Factor Expression**
General Gas Equation	Moody chart or Colebrook Equation $\frac{1}{\sqrt{f_F}} = -4.0 \log_{10}\left(\frac{e/d}{3.7} + \frac{5.02}{\mathrm{Re}\sqrt{f_F}}\right)$
Weymouth	$f_F = \frac{\kappa_W}{d^{1/3}}$
Panhandle-A (Original Panhandle)	$f_F = \frac{\kappa_{PA}}{\left(\frac{q_{Gsc} \cdot SG_G}{d}\right)^{0.1461}}$
Panhandle-B (Modified Panhandle)	$f_F = \frac{\kappa_{PB}}{\left(\frac{q_{Gsc} \cdot SG_G}{d}\right)^{0.03922}}$
AGA (partially turbulent)	$\frac{1}{\sqrt{f_F}} = 4F_D \log_{10}\left(\frac{\mathrm{Re}\sqrt{f_F}}{1.41}\right)$
AGA (fully turbulent)	$\frac{1}{\sqrt{f_F}} = 4.0 \log_{10}\left(\frac{3.7d}{e}\right)$

where: s = dimensionless elevation parameter equal to $0.0375\left(\frac{SG_G \cdot \Delta H}{Z_{av} \cdot T_{av}}\right)$ in customary field units (ΔH in ft, T in R), L_e = pipe equivalent length, defined as $L_e = \frac{(e^s - 1)}{s} L$. Note that s=0, e^s=1, L_e=L for horizontal pipes (ΔH=*0*). For friction factor calculations, $\kappa_W, \kappa_{PA}, \kappa_{PB}$= unit-dependent constants: κ_W=0.008 for d(in) or 0.002352 for d(m); κ_{PA} = 0.01923 for d(in), q_{Gsc} (SCF/D) or 0.01954 for d(m), q(sm^3/d); κ_{PB}=0.00359 for d(in), q_{Gsc} (SCF/D) or 0.00361 for d(m), q(sm^3/d); σ_G = unit-dependent constant for conductivity calculations, where for q_{Gsc}(SCF/D), L(ft), d(in), p(psia), T(R): σ_G= 2,818; for q_{Gsc}(SCF/D), L(miles), d(in), p(psia), T(R): σ_G= 38.784; for SI units, q_{Gsc} ($sm^{3/}$d), L(m), d(m), p(KPa), T(K): σ_G= 574,901. For the AGA equations: F_D = AGA drag factors (0.90-0.97), Re = Reynolds number. e_f =pipe efficiency.

3.2 Compressor Network Equation

A compressor is a major component in a gas network system as it supplies the energy to transport gas from one end to another. The amount of energy input to the gas by the compressor is dependent upon the pressure of gas and flow rate. Horsepower (HP) represents the energy per unit time and it depends on the gas pressure and flow rate and as flow rate increases, the pressure also increases, hence increasing the total HP required.

The head developed by the compressor is defined as the amount of energy supplied to the gas per unit mass of gas. Section 3.2.1 shows the derivation of the compressor equation based of several fundamental properties and assumptions.

3.2.1 Derivation of Compressor Equation for Single-Phase Flow

There are different processes by how gas is compressed and they are categorized as isothermal, adiabatic (isentropic) and polytropic compression. Isothermal compression is a process where the gas pressure and volume are compressed as such that there will be no changes in temperature. Hence, the least amount of work done is through isothermal compression with comparison to other types of gas compression. However, this process is only of theoretical interest since it is virtually impossible to maintain temperature constant while compression is taking place (Menon, 2005).

On the other hand, adiabatic compression is essentially a process defined by zero heat transfer occurring between any molecules in contact with the gas. Isotropic is referred as when an adiabatic process is frictionless. Polytropic compression is intrinsically similar to adiabatic compression, except that there is no need for zero heat transfer in the process. The relationship between pressure and volume for both an adiabatic and a polytropic process is as follows:

$$PV^{n_p} = C \tag{3.9}$$

and

$$P_1V_1^{n_p} = P_2V_2^{n_p} \tag{3.10}$$

where: P = pressure, V= volume, C= constant

n_p = polytropic exponent (polytropic process). Note that $n_p = \gamma$ = ratio of specific heats of gas if the process is adiabatic (isentropic).

Hence, work done by compression could then be calculated by integrating the expression (3.10):

$$W = \int_{p_1}^{p_2} v dp \tag{3.11}$$

where: W = work done by compression. Taking the integral of expression (3.11) then yields, for a polytropic process:

$$W = \frac{n_p}{n_p - 1} p_i v_i \left[\left(\frac{p_j}{p_i} \right)^{\frac{n_p - 1}{n_p}} - 1 \right] \tag{3.12}$$

Since energy could be defined as work done by a force, the power required to run the compressor station could then be expressed in the context of gas flow rate and discharge pressure of compression station:

$$HP = M\,W \tag{3.13}$$

Substituting $M = \rho_{sc} q_{sc}$ and expression (3.12) into expression (3.13), the equation written in terms of Power is as below:

$$HP = \rho_{sc} q_{g_{ij}} \frac{n_p}{n_p - 1} p_i v_i \left[\left(\frac{p_j}{p_i} \right)^{\frac{n_p - 1}{n_p}} - 1 \right] \tag{3.14}$$

where: HP = Power,

M = Mass Flow Rate,

ρ_{sc} = Density at standard conditions

$q_{g_{ij}}$ = Gas Flow Rate

Using real gas law, $pV = ZRT$ can be substituted in the expression (3.14) to account for average compressibility factor effects.

Considering units conversion for oilfield units standard, a rather common form of the formula for multistage compression, which assumes intercooling and equal compression ratios across all stages, is:

$$HP = 0.0857 \frac{n_{st} \cdot n_p}{n_p - 1} q_{G_{ij}} T_i Z_{av} (\frac{1}{\eta}) \left[(\frac{p_j}{p_i})^{\frac{n_p - 1}{n_p \cdot n_{st}}} - 1 \right] \quad (3.15)$$

where:

HP = compressor horsepower, HP

n_p = polytropic coefficient or ratio of specific heats (if adiabatic), dimensionless

n_{st} = number of compression stages,

T_i = suction temperature of gas, R

$q_{G_{ij}}$ = gas flow rate, MMSCFD

P_i = entry suction pressure of gas, psia

P_j = final discharge pressure of gas, psia

Z_{av}= average gas compressibility, dimensionless

η = compressor adiabatic (isentropic) or polytropic efficiency, decimal value (0.75-0.85)

3.3 Wellhead Network Equation

Wells are primarily treated as sources for the natural gas network. Wells are assumed to be producing from a defined shut-in pressure (i.e., reservoir pressure at shut-in conditions adjusted by hydrostatics) and the flow rate is ultimately dependent on prevailing wellhead pressures. The classic backpressure equation relating gas rate to flowing pressure as developed by Rawlins and Schellhardt (1936) is expressed at reservoir conditions as:

$$q_{wGi} = C_R \cdot (p_R^2 - p_{wf}^2)^n \qquad \text{for } 0.5 < n < 1 \tag{3.16}$$

where: C_R = reservoir conductivity or productivity index. The productivity index is only constant when the well is producing in a pseudo-steady state and it could be obtained from well-testing data or isochronal testing of the well. This equation can also be rewritten at surface (wellhead) conditions with the following approximation:

$$q_{wGi} = C_w \cdot (p_{shut}^2 - p_{wh}^2)^n \qquad \text{for } 0.5 < n < 1 \tag{3.17}$$

where C_w = well conductivity. Please note that C_w essentially captures or integrates the effects of the reservoir productivity index and tubing performance using outflow/inflow nodal analysis.

The backpressure equation originated from field observations for a low-pressure gas well, the backpressure coefficient is found to be n=1 as it matches the behavior predicted by Darcy's Law in Equation (3.16). Smaller values of *n* reflect the deviations from Darcy's law that affect the calculations and interpretations of gas well production. The equation was empirically developed after interpreting several hundreds of multi-rate gas wells. A

linear trend was actually scrutinized on the log-log plot of rate versus delta pressure-squared (Golan and Whitson, 1991). It was observed that the pressure squared actually accounts for the fluid properties that are highly dependent on pressure such as the gas viscosity and compressibility factor.

3.4 Newton-Based Gas Network Model

Gas network analysis entails the calculations of flow capacity of each pipeline segment (B-segments) and pressure at each pipe junction (N-nodes) in a network. This can be accomplished either by making pipe flows the primary unknowns of the problem (i.e., the *q*-formulation, or nodal-loop formulation, consisting of "B" unknowns) or by making nodal pressures the primary unknowns (i.e., the *p*-formulation, or nodal formulation with "N-1" unknowns). In looped networks, a Δq-formulation or loop formulation, where loop flow corrections become the primary unknowns in the problem, is also possible. In all cases, in order to achieve mathematical closure, the number of available equations must match the number of unknowns in the formulation.

3.4.1 Nodal-loop or *q*-formulation

In a nodal-loop formulation, network governing equations are articulated via the application of mass conservation principles applied to each *node* and energy conservation principles applied to each *loop* in the system in order to solve for all "*B*" unknowns (i.e., individual pipe flow rates). The approach is known as the "*nodal-loop*" formulation because of the source of the equations being used, but also as a "*q-formulation*" because

of the type of the unknowns being solved for. Mass conservation written at each node requires that the algebraic sum of flows entering and leaving the node must be equal to zero. In other words,

$$\sum q_{Gij}^{in} - \sum q_{Gij}^{out} + S - D = 0 \quad \textit{written for each node and flows converging to it} \qquad (3.18)$$

"N" equations of mass conservation of this type can be written at each nodal junction in the system. Equation (3.18) is recognized as the 1st law of Kirchhoff of circuits, in direct analogy to the analysis of flow of electricity in electrical networks. "*S*" and "*D*" represent any external supply or demand (sink/source) specified at the node. For gas networks, this equation is actually a mass conservation statement even though it is explicitly written in terms of volumetric rates evaluated at standard conditions. Equation (3.18) provides "N-1" admissible equations because only "N-1" nodal equations are linearly independent. In this *nodal-loop* formulation, "LP" additional equations are also needed to exactly balance the number of unknowns "B" [since (N-1) + LP = B] and achieve mathematical closure in the formulation. These equations are formulated by applying the 2nd law of Kirchhoff to every independent loop. In any closed loop, the algebraic sum of all pressure drops must equal zero. This is true of any closed path in a network, since the value of pressure at any point of the network must be the same regardless of the closed path followed to reach the point. The signs of the pressure drops are taken with respect to a consistent sense of rotation around the loop, and the loop equation is written as:

$$\sum_{ij}^{\in loop} (p_i^2 - p_j^2) = 0 \qquad \textit{written for each pipe within any given loop} \qquad (3.19)$$

Following **Table 3.1**, loop equations are rewritten in terms of flow rates using the horizontal pipe flow constitutive equation in terms of pipe conductivities:

$$\sum_{ij}\left(\frac{q_{Gij}}{C_{ij}}\right)^{1/n}=0 \qquad \textit{written for each pipe within any given loop} \tag{3.20}$$

Once mathematical closure has been attained (number of equations = number of unknowns), a mathematical solution strategy is formulated, which is the subject of the solution of network equations section in this manuscript. Please note that the loop-node formulation requires the user to pre-define or identify all flow loops within the system in order to formulate network governing equations.

3.4.2 Loop or Δq-formulation

In a loop formulation, network equations are written in terms of the principles of energy conservation around a loop stated in Equations (3.19) and (3.20) above. The energy conservation equation is given by Kirchhoff's 2nd law which states that sum of pressure drops around any loop is zero. Because only "LP" equations become available in this approach, flow rate corrections (Δq_{loop}) defined for each loop become the unknowns of the formulation as shown below:

$$\sum_{ij}\left(\frac{q_{Gij}^{old}+\Delta q_{loop}}{C_{ij}}\right)^{1/n}=0 \quad \textit{written for each pipe within any given loop} \tag{3.21}$$

Two different sets of flows are defined in a Δq-formulation or loop formulation: branch flows and loop flows. Branch flows (q_{Gij}) are approximations to the true pipe flow values

and loop flows (Δq_{loop}) are introduced to correct prevailing branch flows in order to yield the actual values. Initial values for both branch flow and loop flows are required for the iterative procedure. When Equation (3.21) is satisfied for all loops, convergence has been attained. This formulation also requires the user to identify all flow loops within the network system prior to formulating associated governing equations. Since a number of permutations of independent loops are possible for any given large network, this formulation further requires optimization strategies for the optimal set of loops that would be used during the solution strategy.

3.4.3 Nodal or *p*-formulation

In a nodal formulation, network equations are written on the basis of the principle of nodal mass conservation (continuity) alone. This yields "N-1" linearly independent equations that can be used to solve for "N-1" unknowns (i.e., nodal pressures) since one nodal pressure is assumed to be specified within the system. In this formulation, nodal mass conservation statements in Equation (3.18) are rewritten in terms of nodal pressures using the pipe flow constitutive equations in **Table 3.1**, which yields for horizontal flow:

$$\sum_{ij} C_{ij} \cdot (p_i^2 - p_j^2)^n + S - D = 0 \tag{3.22}$$

In Equation (3.22), fluid flowing into the node is assumed positive and fluid leaving the node is given a negative sign. External supplies and demands (sink/sources) specified at the node are also considered. The p-formulation or nodal method does not require the identification or optimization of loops and the application of the 2nd law of Kirchhoff is circumvented. However in a p-formulation, the resulting set of governing equations is

more complex and more non-linear than the ones found in the loop- and nodal-loop counterparts since pressures are expressed in squared difference. In addition, the method is well-known to suffer from poor convergence characteristics or severe sensitivity to initialization conditions when Newton-Raphson protocols are implemented to achieve a solution (Ayala, 2012; Larock *et al.*, 2000, Osiadacz, 1987).

With that, this study shows that the highly non-linear nodal equations in Equation (3.22) can be readily transformed into linear equations to circumvent this problem. As a result, the poor convergence characteristics of the p-formulation are eliminated, convergence is made independent of user-defined initial guesses for nodal pressures and flow rates, and the needs of calculating expensive Jacobian formulations and associated derivatives are also removed. Concurrently, the analog method which will be discussed below retains the advantages of the p-formulation in terms of not requiring loop identification protocols.

CHAPTER 4

THE LINEAR PRESSURE ANALOG MODEL

4.1 Linear Analog Model

Regardless of the type formulation used, all Newton-based methods are prone to lack of convergence and sensitivity to initial guesses, with the nodal formulation being the most susceptible of all. Presumption of appropriate initial guesses is the key for solving gas network equations for every existing method. In order to circumvent network solution convergence problems of currently available methods and their potentially costly implementation, this study proposes the implementation of a linear-pressure analog model for the solution of the highly non-linear equations in natural gas transportation networks. The method consists of defining an alternate, analog system of pipes that obey a much simpler pipe constitutive equation, i.e., a linear-pressure analog flow equation, which is written for horizontal pipes as follows:

$$q_{Gij} = L_{ij} \cdot (p_i - p_j) \tag{4.1}$$

where L_{ij} is the value of the *linear pressure analog* conductivity. Note that Equation (4.1) uses the flow-pressure drop dependency prescribed by the Hagen-Poiseuille's law for liquid flow in laminar conditions. Consequently, the proposed analog seeks to map the highly non-linear gas flow network problem into the much more tractable liquid network problem for laminar flow conditions. When gas pipe flows are written in terms of such a linear pressure analog, nodal mass balances used in p-formulations (Equation 3.22)

collapse to a much simpler (and more importantly, linear) set of algebraic equations shown in Equation (4.2):

$$\sum L_{ij} \cdot (p_i - p_j) + S - D = 0 \tag{4.2}$$

which can be simultaneously solved for all nodal pressures in the network using any standard method of solution of *linear* algebraic equations—as opposed to its non-linear counterpart of Equation (3.22).

Linear-pressure analog conductivities are straightforwardly calculated as a function of actual pipe conductivities according to the following transformation rule:

$$L_{ij} = T_{ij} \cdot C_{ij} \tag{4.3}$$

where L_{ij} is the conductivity of the *linear-pressure analog* pipe which conforms to the linear equation in (4.1), and C_{ij} is the actual pipe conductivity conforming to the generalized flow equation definition in **Table 3.1** that for horizontal pipes becomes:

$$q_{Gij} = C_{ij} \cdot (p_i^2 - p_j^2)^n \tag{4.4}$$

In Equation (4.4), n is equal to 0.50 as prescribed by the generalized gas flow equation. It is straightforwardly demonstrated that the variable T_{ij} in Equation (4.3), i.e., the analog-pipe conductivity transform, is given by the expression:

$$T_{ij} = \sqrt{1 + \frac{2}{r_{ij} - 1}} \tag{4.5}$$

This analog-pipe transform is a dimensionless quantity that enforces the flow-rate equivalency of Equations (4.1) and (4.4) for the pipe of interest. The dimensionless

analog-pipe transform turns out to be solely dependent on r_{ij}, i.e., the pressure ratio between the pipe end pressures as shown in Equation (4.6):

$$r_{ij} = \frac{p_i}{p_j} \tag{4.6}$$

where i=upstream node and j=downstream node as defined in Equations (4.1) and (4.4). The derivation of linear-pressure analog conductivity is shown in **Figure 4.1** below.

$$q_{Gij} = L_{ij}(p_i - p_j) \qquad q_{Gij} = C_{ij}(p_i^2 - p_j^2)^{0.5}$$

$$L_{ij}(p_i - p_j) = C_{ij}(p_i^2 - p_j^2)^{0.5}$$

$$\frac{L_{ij}}{C_{ij}} = \frac{(p_i - p_j)(p_i + p_j)}{(p_i - p_j)(p_i^2 - p_j^2)^{0.5}}$$

$$\frac{L_{ij}}{C_{ij}} = \left(\frac{\frac{p_i}{p_j} + 1}{\frac{p_i}{p_j} - 1}\right)^{0.5} \qquad Let\ r_{ij} = \frac{p_i}{p_j}$$

$$\frac{L_{ij}}{C_{ij}} = \left(\frac{r_{ij} + 1}{r_{ij} - 1}\right)^{0.5}$$

$$\frac{L_{ij}}{C_{ij}} = \sqrt{1 + \frac{2}{r_{ij} - 1}} \qquad Let\ T_{ij} = \sqrt{1 + \frac{2}{r_{ij} - 1}}$$

$$L_{ij} = T_{ij} C_{ij}$$

Figure 4.1: Derivation of Linear-Pressure Analog Conductivity

Because pressure ratios are always higher than one ($p_i > p_j$ for fluid to flow, given that the *i-th* node is always defaulted to the upstream location), analog-pipe transforms are constrained to take values larger than unity. **Figure 4.2** illustrates this dependency for a variety of pressure ratios. Since $T_{ij} > 1$, it follows that $L_{ij} > C_{ij}$ from the transformation rule in equation (4.3). Resulting linear-analog conductivities have larger values than actual pipe conductivity, i.e., linear-analog pipes are more "conductive" than their gas counterparts in terms of absolute conductivity values. In general, L_{ij}'s at least double C_{ij}'s in most networks, given that pipes rarely operate at very large r_{ij}'s since energy losses would be excessive for an economical operation.

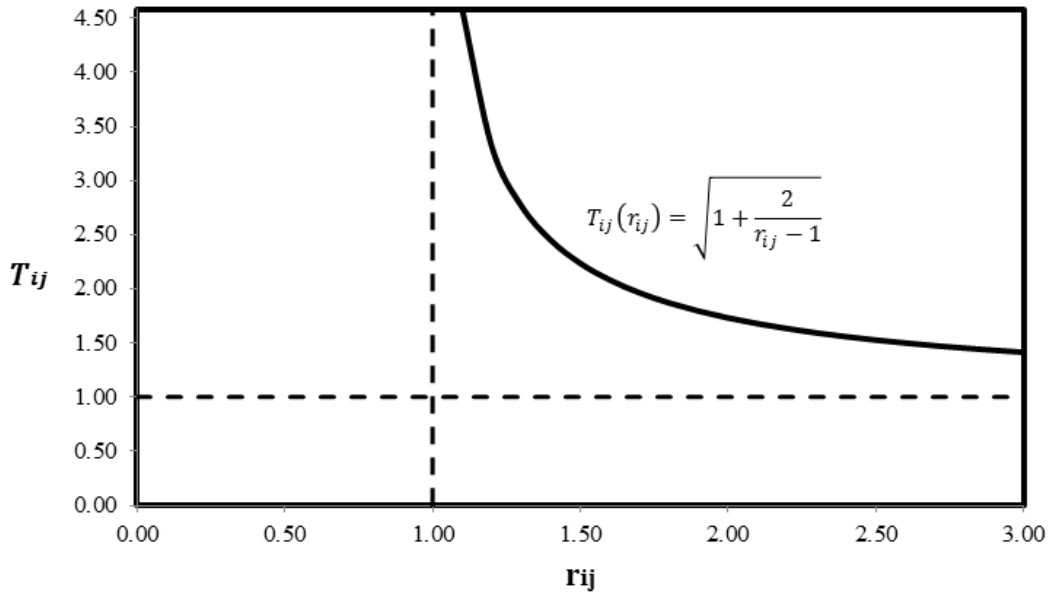

Figure 4.2: Analog-pipe conductivity transform (T_{ij}) as a function of pipe pressure ratio (r_{ij})

Once the linear-analog transform has been applied, all unknown nodal pressures in the network can be calculated by solving the resulting linear set of algebraic equations. Since actual pressure ratios (r_{ij}) are not known in advance, the linear analog method starts its first iteration with the condition $L_{ij} = C_{ij}$. Note that no initial guesses for nodal pressure values or pipe flow rates are needed. However, once a first set of estimated nodal pressures become available during the first iteration, interim pressure ratios (r'_{ij}), pipe conductivities, and pipe flow rates can be calculated. In this first iteration, resulting pressure drops would become significantly overestimated because pipe analogs are forced to be less conductive than they should since $L_{ij} > C_{ij}$ instead of $L_{ij} = C_{ij}$. Interim pressure ratios (r'_{ij}) thus start at significantly overstated values during the first iteration and, upon successive substitutions and after a few inexpensive iterations, they steadily adjust to actual r_{ij}. When this occurs, the non-linear network problem has been fully solved. Convergence is attained when any further nodal pressure update would become inconsequential within a prescribed tolerance (e.g. $\varepsilon < 10^{-3}\ psia$).

Because pressure drops are always overestimated in the first analog iterations, upstream pressures will be underestimated if downstream pressures are specified. This may force upstream pressure to take negative values early during the iterative procedure. For these cases, a direct application of Equation (4.6) would violate the analog principle that requires all pipe pressure ratios to be positive and higher than 1. Therefore, if negative downstream pressure is calculated, Value of pressure ratio calculations is defaulted to a

minimum value (equal to atmospheric pressure) and upstream pressure is displaced accordingly using the calculated pipe pressure drop. In other words,

$$r_{ij} = \frac{|(p_i - p_j)| + 14.7}{14.7} \tag{4.7}$$

Please note that this type of adjustment can be avoided altogether if instead of initializing the analog method with the condition $L_{ij} = C_{ij}$ (first iteration), one uses a multiple of the pipe conductivity (such as $L_{ij} = 2C_{ij}$ or $L_{ij} = 3C_{ij}$) for initialization. Such initialization makes the linear analog more conductive from the onset, thus avoiding unnecessarily large pressure loss estimations during the first iteration.

It can be shown that the proposed analog method has a remarkably stable performance. This is due in part because its iterations do not necessitate user-prescribed guesses and each individual iteration solves a feasible liquid-flow scenario with a unique solution. This is to be compared to the potentially unconstrained behavior of Newton-Raphson protocols, which demand the use of good initializations (i.e., initial "guesses" sufficiently close to the actual solution) for convergence to be possible. The proposed approach is also fundamentally different from the Linear Theory method (Wood and Carl, 1972) in the sense that it always relies on exact solutions to well-behaved linear-analog liquid fluid flow problems for each of its iterations. The Linear Theory Method, instead, relies on solving approximate sets of linearized equations, which do not necessarily correspond

to physically-constrained systems and thus is susceptible to spurious numerical oscillations.

Note that the value of C_{ij} in the transformation in Equation (4.3) remains constant during the iteration process for all flow equations where friction factor (and thus pipe conductivity as per its definition in **Table 3.1**) are defined to be independent of flow rate. This is the case, for example, of the Weymouth and the AGA fully-turbulent friction factor equations in **Table 3.1**. For all other flow-rate-dependent friction factor equations, in order to preserve initial-guess-free nature of the solution process, the C_{ij} estimation is defaulted to that of flow-rate independent flow equation such as Weymouth. For all subsequent iterations, C_{ij} becomes simultaneously updated based on the most current flow rate information using the friction factor expression of choice from **Table 3.1**. The proposed workflow for the implementation of the linear-analog methodology is displayed in **Figure 4.3**.

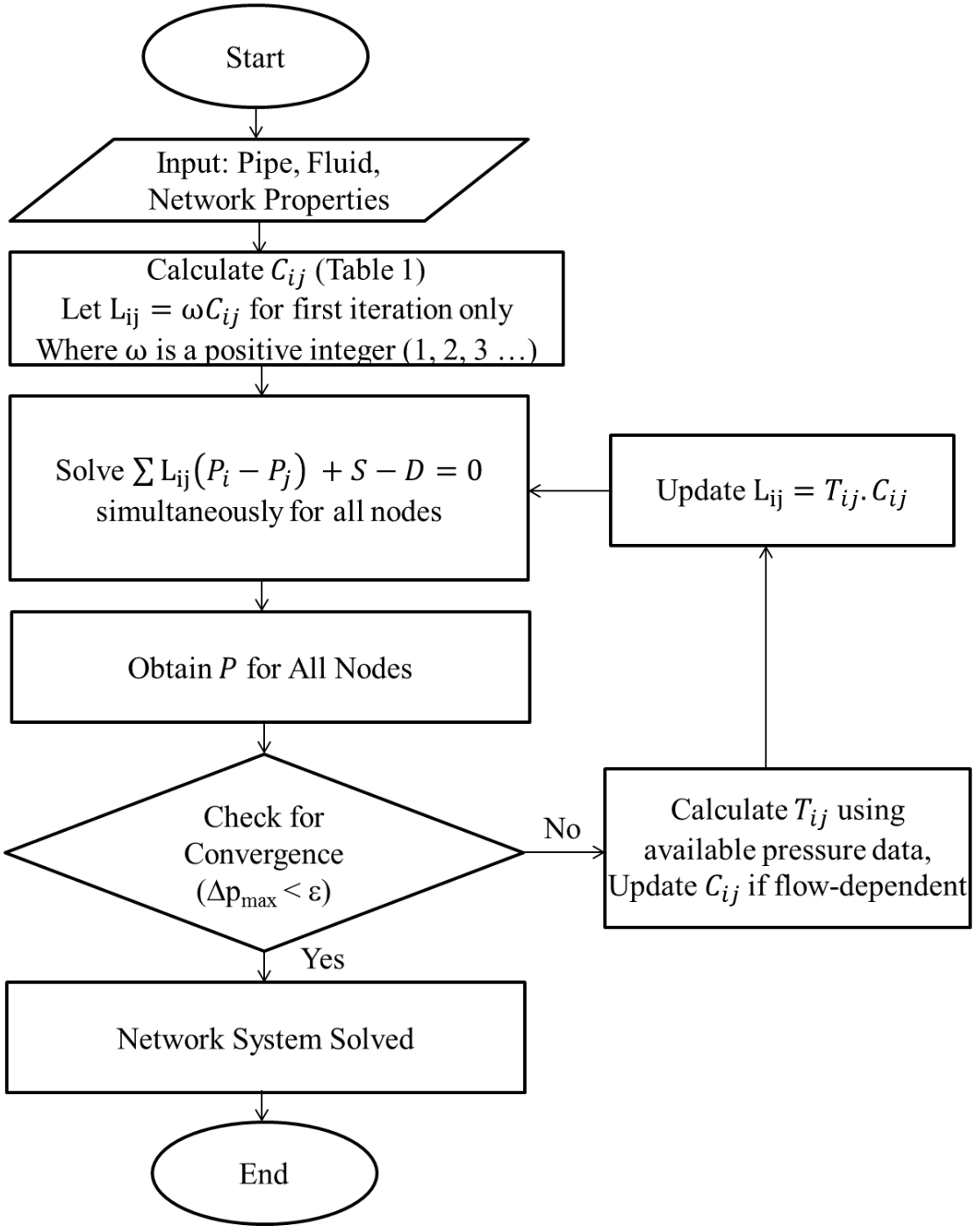

Figure 4.3: Flow Chart for Linear-Analog Implementation

4.1.1 Extension to Networks with Inclined-Pipes

Similar analog transformations can be proposed to extend the linear-analog model to network systems with inclined pipes. The constitutive gas flow equation (4.4) for inclined pipes becomes

$$q_{Gij} = C_{ij} \cdot (p_i^2 - e^{s_{ij}} p_j^2)^{0.5} \tag{4.8}$$

where s is the pipe elevation parameter, n is equal to 0.50, and C_{ij} is the actual pipe conductivity for the inclined generalized flow equation definition shown in **Table 3.1**. On the basis of this constitutive equation, the linear pressure analog model for inclined pipe systems is postulated as:

$$q_{Gij} = L_{ij}\left(p_i - e^{\frac{s}{2}} p_j\right) \tag{4.9}$$

which leads to the same analog-pipe conductivity transform in Equation (4.5):

$$T_{ij} = \sqrt{1 + \frac{2}{r_{ij} - 1}} \tag{4.10}$$

but with a slightly modified definition of the pressure ratio for inclined pipes given by:

$$r_{ij} = \frac{p_i}{e^{\frac{s}{2}} p_j} \tag{4.11}$$

Note that the analog-pipe conductivity transform for inclined pipes is identical to that of horizontal pipes, and only the pressure ratio definition is slightly modified with the elevation correction for the downstream pressure. The resulting characteristic matrix **K,** as discussed in Chapter 5 Results and Discussions, would be asymmetric due to the elevation correction introduced in the linear analog model.

However, it is also possible to redefine the linear-analog transform for inclined pipes in order to preserve the symmetry of the characteristic matrix **K**, whenever desired, if the application of efficient Cholesky algorithms is deemed of importance. Characteristic matrix symmetry can be preserved by implementing the analog constitutive equation in Equation (4.1) for inclined pipes, reproduced below:

$$q_{Gij} = L_{ij} \cdot (p_i - p_j) \tag{4.12}$$

which would lead to a different analog-pipe conductivity transform than the one used thus far:

$$T_{ij} = \sqrt{\frac{r_{ij}^2 - e^{s_{ij}}}{(r_{ij}-1)^2}} \tag{4.13}$$

and which uses the same conventional pressure ratio definition:

$$r_{ij} = \frac{p_i}{p_j} \tag{4.14}$$

This alternative approach would lead to linear algebraic equations with a symmetric characteristic matrix. All proposed analog methods are summarized in the **Table 4.1** below.

Table 4.1: Summary of Linear-Pressure Analog Constitutive Equations ($L_{ij} = C_{ij} \cdot T_{ij}$)

Network Type	**Linear-Pressure Analog Constitutive Equation**	**Analog Conductivity Transform, T_{ij}**
Horizontal Pipes *(for a symmetric characteristic matrix)*	$q_{Gij} = L_{ij}(p_i - p_j)$	$T_{ij} = \sqrt{1 + \frac{2}{r_{ij} - 1}}$, $where\ r_{ij} = \frac{p_i}{p_j}$

Inclined Pipes - Approach 1 *(for an asymmetric characteristic matrix)*	$q_{Gij} = L_{ij}(p_i - e^{\frac{s_{ij}}{2}} p_j)$	$T_{ij} = \sqrt{1 + \frac{2}{r_{ij} - 1}}$, $where\ r_{ij} = \frac{p_i}{e^{\frac{s_{ij}}{2}} p_j}$
Inclined Pipes - Approach 2 *(for a symmetric characteristic matrix)*	$q_{Gij} = L_{ij}(p_i - p_j)$	$T_{ij} = \sqrt{\frac{r_{ij}^{\,2} - e^{s_{ij}}}{(r_{ij} - 1)^2}}$, $where\ r_{ij} = \frac{p_i}{p_j}$

4.1.2 Extension to Networks with Compressors

As discussed in Chapter 3.2, the compressor equation is given by:

$$HP = 0.0857 \frac{n_{st} \cdot n_p}{n_p - 1} q_{G_{ij}} T_i Z_{av} (\frac{1}{\eta}) \left[(\frac{p_j}{p_i})^{\frac{n_p - 1}{n_{st} \cdot n_p}} - 1 \right] \tag{4.15}$$

Since the linear analog model is developed based upon the nodal formulation and the network formulation is based upon the principle of nodal mass continuity, the compressor equation is then written in terms of pipe flow constitutive equations.

Rearranging the compressor equation at a short-hand equation, one obtains:

$$q_{G_{ij}} = \frac{HP}{k_c \left[(r_{C_{ij}})^{\frac{n_p - 1}{n_{st} \cdot n_p}} - 1 \right]} \tag{4.16}$$

where:

$$k_c = 0.0857 (\frac{n_{st} \cdot n_p}{n_p - 1}) T_i (Z_{av}) (\frac{1}{\eta}) \tag{4.17}$$

The total compressor ratio for a compression station is calculated as the ratio of its final compressor discharge pressure to its entry suction pressure:

$$r_{c_{ij}} = \frac{p_j}{p_i} \tag{4.18}$$

In order to construct linear sets of equations from coupling compressors, the compression ratio is assumed to be the target variable that needs to be specified by the user. For such scenarios,

$$q_{G_{ij}} = C_{cij}.HP \tag{4.19}$$

where the compressor constant is given as:

$$C_{cij} = \frac{1}{k_c\left(\left(r_{cij}\right)^{\frac{n_p-1}{n_{st}\cdot n_p}} - 1\right)} \text{ [MMSCD/HP]} \tag{4.20}$$

The compressor equation is then incorporated into the gas network system by predefining the compressor desired total compression ratio, which results in the determination of the horsepower required for the compressor to be solved for as an unknown within the system of equations.

4.1.3 Extension to Networks with Wellheads

The wellhead equation at surface (wellhead) conditions can be written as:

$$q_{wG_i} = C_w.(p_{shut}{}^2 - p_{wh}{}^2)^n \qquad \text{for } 0.5 < n < 1 \tag{4.21}$$

This constitutive relationship retains a form identical to that of the pipeline gas flow equation and hence a similar analog transformation could be applied to linearize the wellhead equation. The backpressure equation is similar to the way the generalized pipe equation is expressed, while the coefficients n and C_w vary for different reservoir and tubing properties for the backpressure equation.

The linear analog equation for any wellhead in the network system is then given by:

$$q_{wGi} = L_w \cdot (p_{shut} - p_{wh}) \tag{4.22}$$

Linear-pressure analog conductivities for a wellhead are again computed as a function of actual well conductivities according to the following transformation rule:

$$L_w = T_w \cdot C_w \tag{4.23}$$

where L_w is the wellhead conductivity in the *linear-pressure analog* model which conforms to the linear equation in (4.22), and C_w is the actual well conductivity conforming to the wellhead equation (4.21). The analog-well conductivity transform T_w in Equation (4.23) now becomes a function of the well flow exponent (which ranges from 0.5 to 1) and the well shut-in pressure, as shown below:

$$T_w = (1-\frac{1}{r_w})^{n-1} \cdot (1+\frac{1}{r_w})^{n} \cdot p_{shut}^{2n-1} \tag{4.24}$$

where the wellhead pressure ratio, r_w is given by the ratio of shut-in pressure, p_{shut} to wellhead pressure, p_{wh} .

$$r_w = \frac{p_{shut}}{p_{wh}} \tag{4.25}$$

Since r_w is not available until the next iteration, L_w is to be approximated by the following expression during the first iteration:

$$L_w = p_{shut}{}^{2n-1} \cdot C_w \tag{4.26}$$

Please note that $p_{shut}{}^{2n-1}$ is the constant that appears in the T_w term and hence it should be introduced in the first iteration to ensure a reasonable conductivity approximation in the first iteration.

Figure 4.4 depicts the dependency of the analog-well conductivity transform for a range of flow exponents. Since $T_w > 1$, it follows that $L_{ij} > C_{ij}$ from the transformation rule in equation (4.23). Similarly, resulting linear-analog conductivities have larger values than actual well conductivity, i.e., linear-analog wells are more "conductive" or "productive" than their gas counterparts in terms of the absolute values of their conductivity. In **Figure 4.4,** P_{shut} was assumed to be 100 psia for illustration purposes.

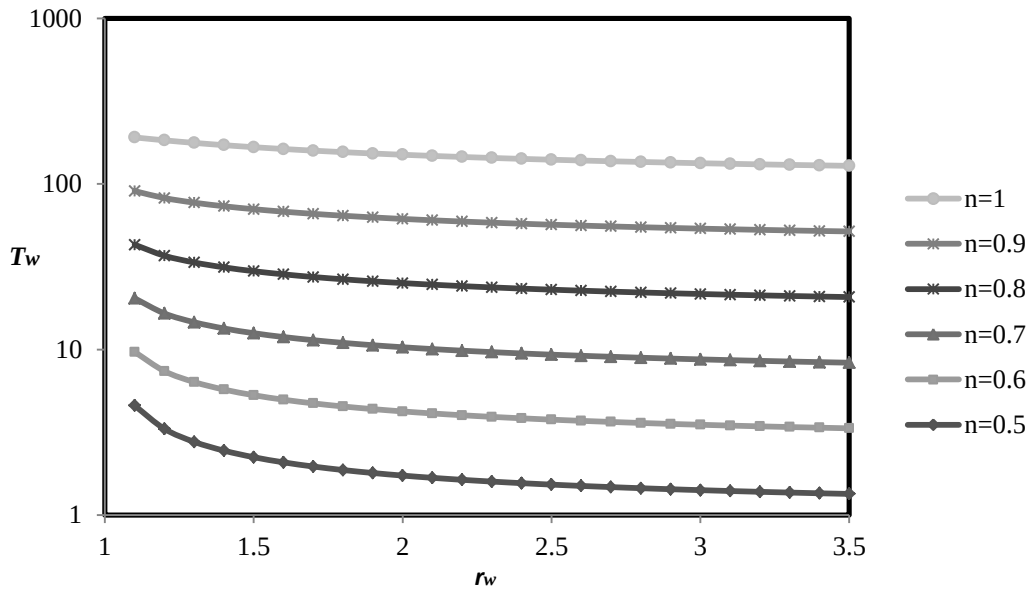

Figure 4.4 Analog-well conductivity transform (T_w) as a function of well pressure ratio (r_w) (for P_{shut} = 100 psia)

Similar to the discussion for pipes, there may be occasions where wellhead pressures can be estimated to be negative during the first iterations. This is due to the fact that early analogs tend to overestimate actual pressure drops in the system. For these cases, since pressure ratios must always be positive and higher than one, the following expression is used when wellhead pressure is deemed to be negative by early iterations:

$$r_w = \frac{p_{shut}}{14.7} \tag{4.27}$$

CHAPTER 5

RESULTS AND DISCUSSIONS

5.1 Case Study 1: Horizontal Pipe Network System

For this case study, the horizontal network system depicted on **Figure 1.1** is analyzed using the generalized gas flow equation coupled with AGA-fully turbulent friction factor calculations. An average flowing temperature of 75 ℉ and an average compressibility factor of 0.90 are assumed for the entire system for illustration purposes; however, the methodology would remain unchanged if each pipe were to be considered to operate at different average temperatures and if compressibility factors were calculated in terms of standard natural gas correlations. Those variables would only affect the update of actual pipe conductivities C_{ij} described in the solution protocol of **Figure 4.3**. The network handles a gas with a specific gravity of 0.69 and all pipes are assumed to be carbon steel (e = 0.0018 in), horizontal, 30-miles long and NPS 4 Sch 40, except for pipes (1,2), (2,3), (1,4) and (4,7) which are NPS 6 Sch 40. The pressure specification is given at node 9 and it is set at 130 psia. Based on the implementation of the solution protocol in **Figure 4.3**, the gas network under study generates the following linear system of algebraic equations in terms of nodal pressures:

$$\begin{bmatrix} -O_1 & L_{12} & 0 & L_{14} & 0 & 0 & 0 & 0 & 0 \\ L_{12} & -O_2 & L_{23} & 0 & L_{25} & 0 & 0 & 0 & 0 \\ 0 & L_{23} & -O_3 & 0 & 0 & L_{36} & 0 & 0 & 0 \\ L_{14} & 0 & 0 & -O_4 & L_{45} & 0 & L_{47} & 0 & 0 \\ 0 & L_{25} & 0 & L_{45} & -O_5 & L_{56} & 0 & L_{58} & 0 \\ 0 & 0 & L_{36} & 0 & L_{56} & -O_6 & 0 & 0 & L_{69} \\ 0 & 0 & 0 & L_{47} & 0 & 0 & -O_7 & L_{78} & 0 \\ 0 & 0 & 0 & 0 & L_{58} & 0 & L_{78} & -O_8 & L_{89} \\ 0 & 0 & 0 & 0 & 0 & 0 & 0 & 0 & 1 \end{bmatrix} \begin{bmatrix} p_1 \\ p_2 \\ p_3 \\ p_4 \\ p_5 \\ p_6 \\ p_7 \\ p_8 \\ p_9 \end{bmatrix} = \begin{bmatrix} -16 \\ 2 \\ 2 \\ 3 \\ 1 \\ 2 \\ 2 \\ 2 \\ 130 \end{bmatrix}$$

which, in compact notation, could be expressed as:

$$\mathbf{K\,P = S}$$

where **K** is the network characteristic matrix, **P** is the network pressure vector and **S** is the network supply/consumption vector. In the **K** matrix, the diagonal entries O_i represent the summation of all off-diagonal entries for the *i-th* row. For instance, $O_1 = L_{12} + L_{14}$; $O_5 = L_{25} + L_{45} + L_{56} + L_{58}$; and $O_8 = L_{58} + L_{78} + L_{89}$. All pipe conductivities (L_{ij} and C_{ij}) are assumed in MMSCFD/psi in this example. Given that what results is a system of linear equations, solution of the matrix equations is simple and straightforward. It could be directly solved using LU decomposition, Gaussian Elimination, Conjugate Gradient methods or any linear equation solver.

Brebbia and Ferrante (1983) present a streamlined protocol for the assembly of the network characteristic matrix and supply/consumption vector for the analysis of a water network under laminar flow, which becomes fully applicable for the assembly of the proposed natural gas linear-analogs. It is shown that the characteristic matrix of the network **K** is straightforwardly constructed in terms of a connectivity table (which

matches each pipe branch with its upstream and downstream nodes) available from input data. This assembly protocol streamlines the identification of the location of each pipe conductivity contribution within the characteristic matrix as a function of the information in the connectivity table. The assembly protocol also honors the presence of boundary conditions, such as pressure and supply/demand specifications. It is recognized that the matrix **K** is a banded matrix, which is a property that can be used to save storage space during computations. The half-bandwidth of this matrix is a function of the maximum difference in the numbers of any two nodes connected to each other; in particular, the half bandwidth is equal to that maximum difference plus one because of the presence of the diagonal. From **Figure 1.1**, this maximum difference is equal to 3, corresponding to the difference between the node numbers of pipes (5,8) or (1,4) for instance. This yields a half-bandwidth of 4 which is evident in the matrix above. A properly numbered large network system can be made to have small half-bandwidths, thus making large storage savings possible.

By moving all known pressure-node matrix entries (L_{69} and L_{89}) to the consumption vector, the characteristic matrix can also become fully symmetric, i.e., $\mathbf{K} = \mathbf{K}^T$. This property can not only be used to save additional storage space (i.e., only the upper or lower portion of the matrix needs to be stored) but also to implement efficient linear equation solvers that fully exploit this property. A system of linear equations with a positive-definite and symmetric matrix can be efficiently and inexpensively solved using Cholesky decomposition, which can be shown to be roughly twice as efficient as LU

decomposition for solving systems of linear equations (Press *et al.*, 2007). Matrix **K** is positive-definite because it is symmetric and diagonally-dominant with positive diagonal entries. Note that positive diagonal entries are obtained by multiplying all matrix and right-hand-side vector entries by -1 for all equations other than the dummy constant-pressure specification.

The inexpensive, steady convergence nature of the proposed protocol is depicted in **Figures 5.1.1 to 5.1.5** for the iterative solution of the case under study. The final converged solution is provided in **Figure 5.1.6**, which fully satisfies the original set of highly non-linear gas network equations. Note, again, that no user-provided guesses of pressure or flow rate are needed at any point of the protocol and that just a few inexpensive iterations are needed for the protocol to reach the immediate neighborhood of the actual solution. **Figure 5.1.1** demonstrates that the values of analog-pipe conductivity transform ratios steadily converge to their true values as the number of iterations increases. This can be further visualized in **Figure 5.1.2,** where it becomes evident that pipe pressure ratios progressively stabilize as the number of iteration increases. The relationship between the analog-pipe conductivity transforms and pressure ratios (originally illustrated in **Figure 4.3**) is continuously honored during the process as demonstrated by **Figure 5.1.3**. As a result, nodal pressures and flow rates steadily approach their true values as the protocol progresses, as shown in **Figure 5.1.4** and **Figure 5.1.5**, respectively. These figures demonstrate that nodal pressures and flow rates are initially overestimated because linear analog conductivities were initially made equal

to actual pipe conductivities. This significantly underestimates linear-analog conductivities and artificially creates initially large pressure drops in the linear-analog model.

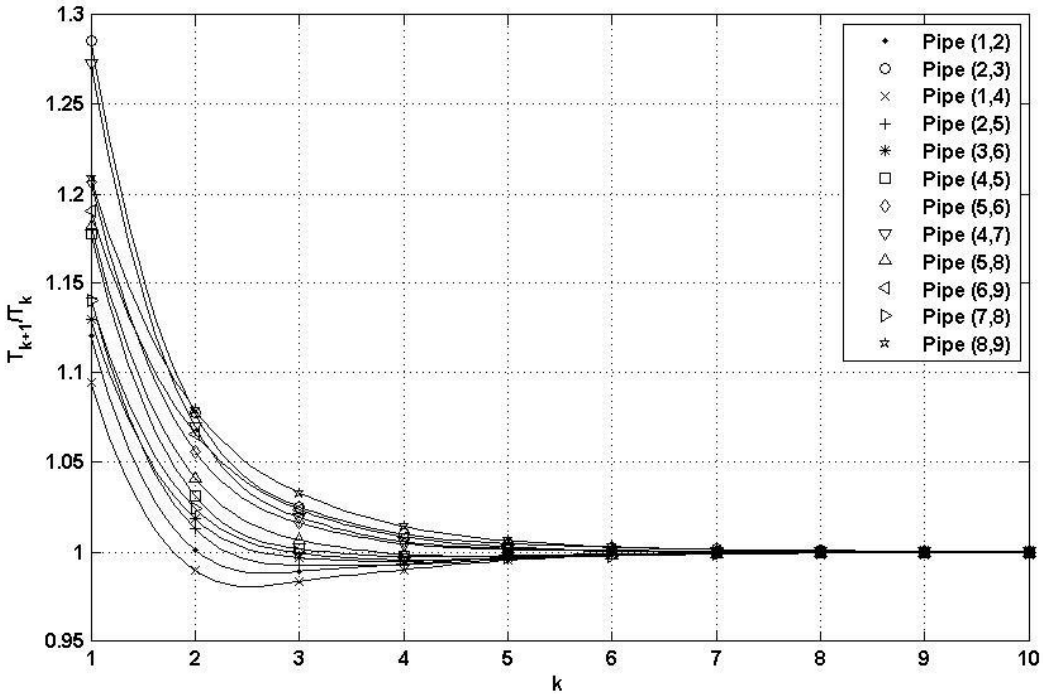

Figure 5.1.1: Analog-pipe conductivity transform improvement ratio (T_{k+1}/T_k) vs. no. of iterations (k) – Case Study 1

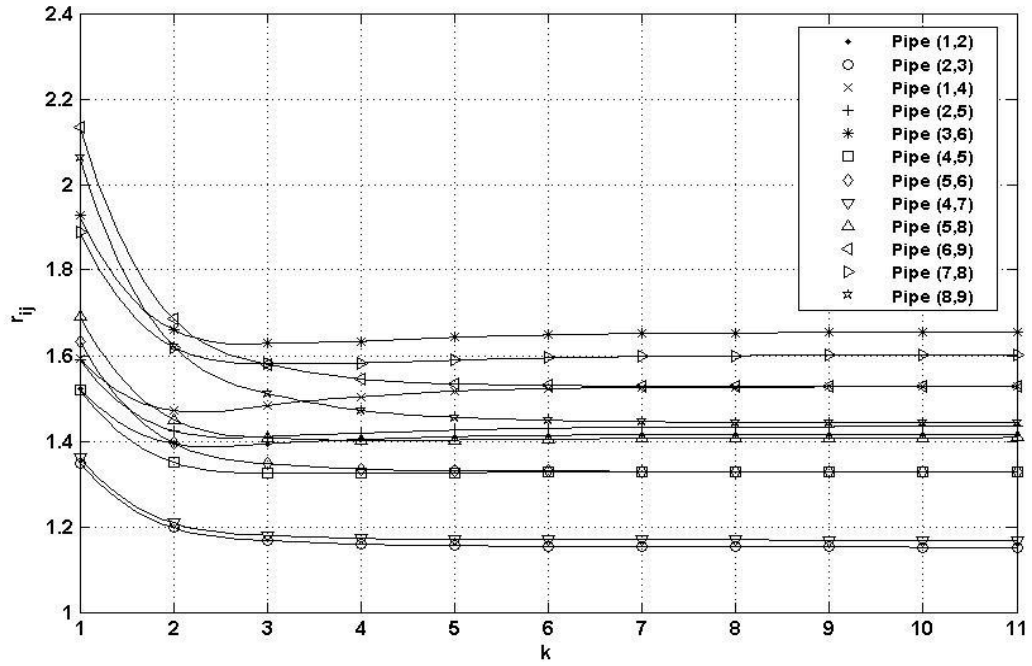

Figure 5.1.2: Pressure ratio (r_{ij}) vs. no. of iterations (k) – Case Study 1

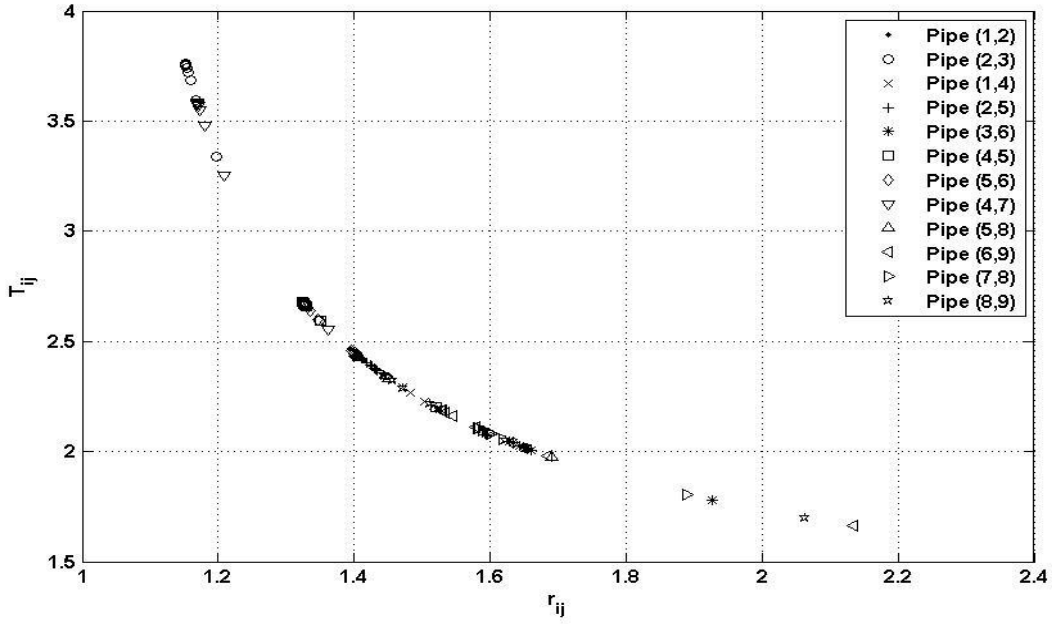

Figure 5.1.3: Analog-pipe conductivity transform (T_{ij}) vs. pressure ratio (r_{ij}) – Case Study 1

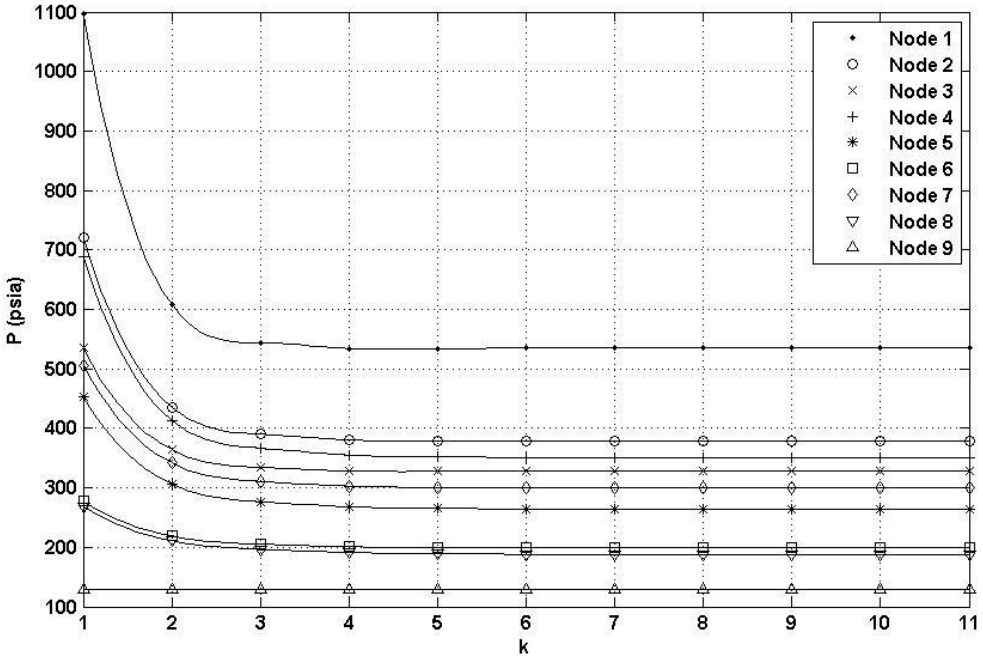

Figure 5.1.4: Nodal pressures (p_i) vs. no. of iterations (k) – Case Study 1

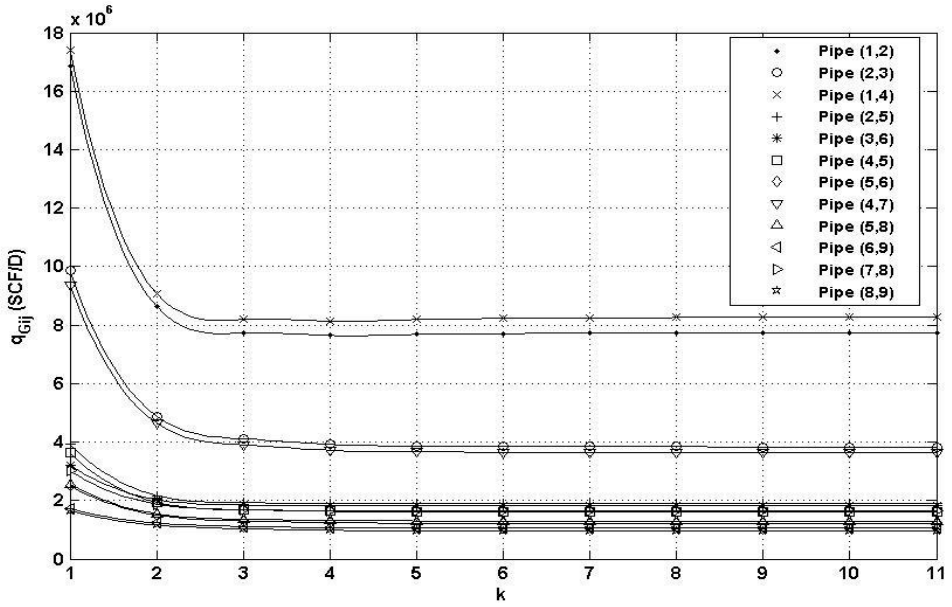

Figure 5.1.5: Pipe flow rate (q_{Gij}) vs. no. of iterations (k) – Case Study 1

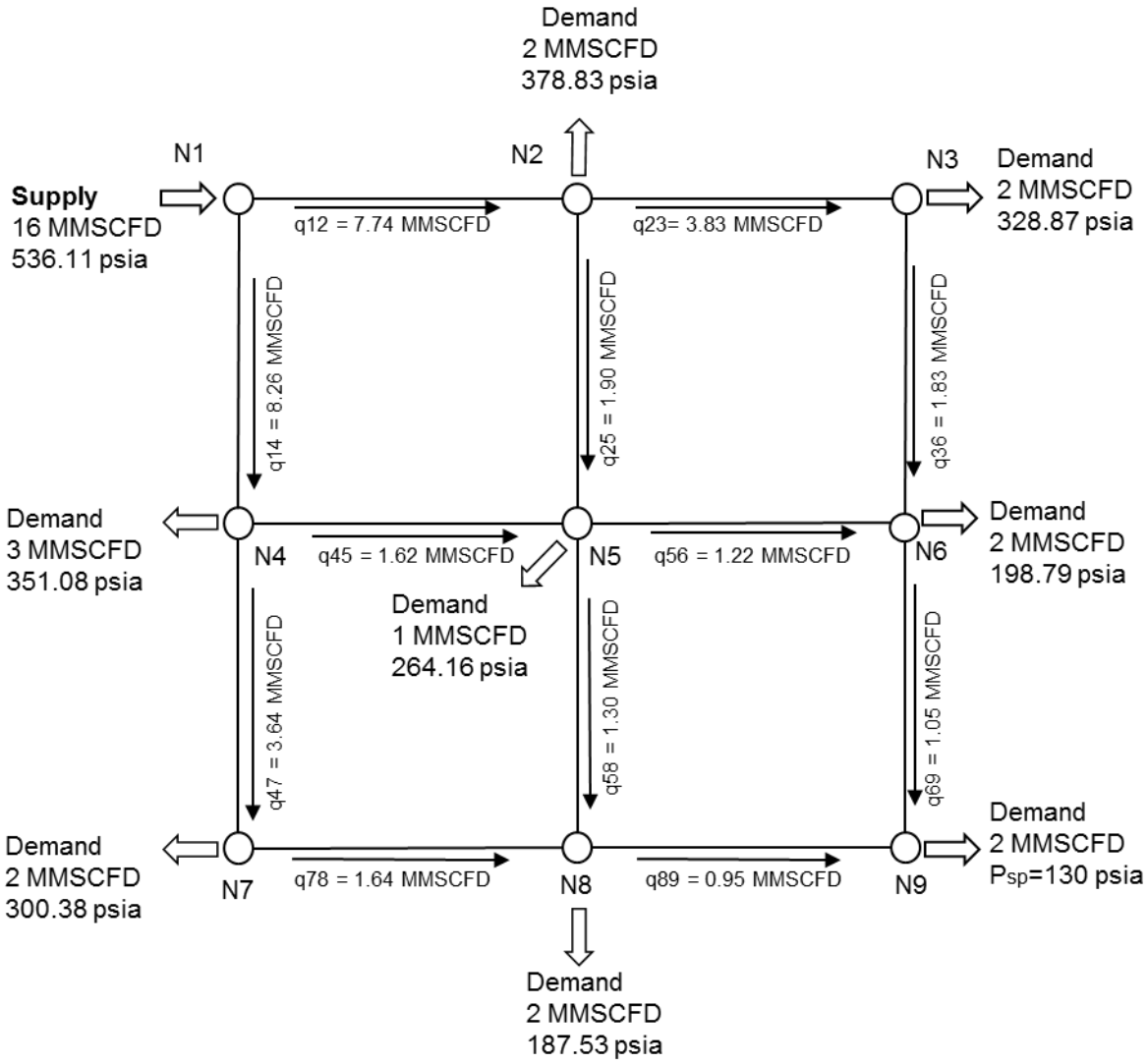

Figure 5.1.6: Fully-converged natural gas network distribution scenario – Case Study 1

5.2 Case Study 2: Inclined Pipe Network System

Case Study 2 considers an identical network and scenario as the one presented in Case Study 1 (illustrated in **Figure 1.1**), but after placing all nodes at different elevations. Reference node 9 is placed at datum level (Elevation=0) and its pressure remains

specified at 130 psia. This case study seeks to incorporate the effect that elevation losses or gains can have on the system into the linear-analog model, which was neglected in the previous case study. Nodal elevation information is provided in **Figure 5.2**.

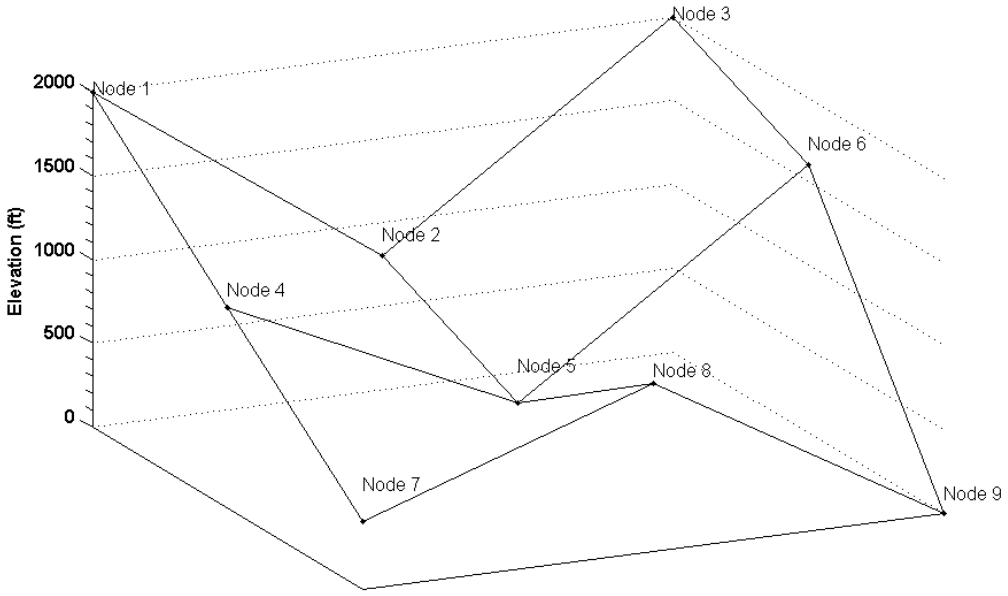

Figure 5.2: Node Elevations for Case Study 2

Based on the implementation of the solution protocol in **Figure 4.3**, the application of the linear-pressure analog constitutive equation in (4.9) for elevated pipes to the gas network under study generates the following linear system of algebraic equations:

$$\begin{bmatrix} -O_1 & e^{s_{12}/2}L_{12} & 0 & e^{s_{14}/2}L_{14} & 0 & 0 & 0 & 0 & 0 \\ L_{12} & -O_2 & e^{s_{23}/2}L_{23} & 0 & e^{s_{25}/2}L_{25} & 0 & 0 & 0 & 0 \\ 0 & L_{23} & -O_3 & 0 & 0 & e^{s_{36}/2}L_{36} & 0 & 0 & 0 \\ L_{14} & 0 & 0 & -O_4 & e^{s_{45}/2}L_{45} & 0 & e^{s_{47}/2}L_{47} & 0 & 0 \\ 0 & L_{25} & 0 & L_{45} & -O_5 & e^{s_{56}/2}L_{56} & 0 & e^{s_{58}/2}L_{58} & 0 \\ 0 & 0 & L_{36} & 0 & L_{56} & -O_6 & 0 & 0 & e^{s_{69}/2}L_{69} \\ 0 & 0 & 0 & L_{47} & 0 & 0 & -O_7 & e^{s_{78}/2}L_{78} & 0 \\ 0 & 0 & 0 & 0 & L_{58} & 0 & L_{78} & -O_8 & e^{s_{89}/2}L_{89} \\ 0 & 0 & 0 & 0 & 0 & 0 & 0 & 0 & 1 \end{bmatrix} \begin{bmatrix} p_1 \\ p_2 \\ p_3 \\ p_4 \\ p_5 \\ p_6 \\ p_7 \\ p_8 \\ p_9 \end{bmatrix} = \begin{bmatrix} -16 \\ 2 \\ 2 \\ 3 \\ 1 \\ 2 \\ 2 \\ 2 \\ 130 \end{bmatrix}$$

which, in compact notation, is expressed as:

$$\mathbf{K\,P = S}$$

In the new **K** characteristic matrix, the upper right portion of the matrix contains all the "$e^{sij/2}$" elevation corrections applicable to downstram nodes and the lower left portion of the matrix contains conductivity information for the upstream nodes. Diagonal entries O_i are no longer just the summation of all off-diagonal entries, given that elevation terms must be taken into account for all cases where node "*i*" is found in the downstream position. For instance, $O_1 = L_{12} + L_{14}$; but $O_5 = L_{25}\, e^{s25/2} + L_{45}\, e^{s45/2} + L_{56} + L_{58}$; and $O_8 = L_{58}\, e^{s58/2} + L_{78}\, e^{s78/2} + L_{89}$. All pipes conductivities (L_{ij} and C_{ij}) remain in MMSCFD/psi in this example. The resulting characteristic matrix **K** remains banded but no longer symmetric; therefore, the implementation of a Cholesky decomposition is no longer possible. The resulting system of linear equations is then directly solved using any other standard linear equation solver such as LU decomposition, Gaussian Elimination, or Conjugate Gradient methods. **Figure 5.2.1 to 5.2.5** present the results of such iterative solution protocol which follows the workflow of **Figure 4.3**. Final converged values or the actual network solution are displayed in **Figure 5.2.6**. As previously shown, analog

conductivity and pressure ratios steadily converge to true values (**Figure 5.2.1** and **5.2.2**, respectively) and maintain the same functional dependency among them (**Figure 5.2.3**). Pressure and flow rate estimations converge steadily and progresively as highlighted in **Figures 5.2.4 and 5.2.5**, respectively. Again, flow rate and pressures are initially overestimated at the beginning because of the actual pipe conductivity are used in the linear analog constitutive equation for the first iteration. Convergence behavior remains smooth and steady.

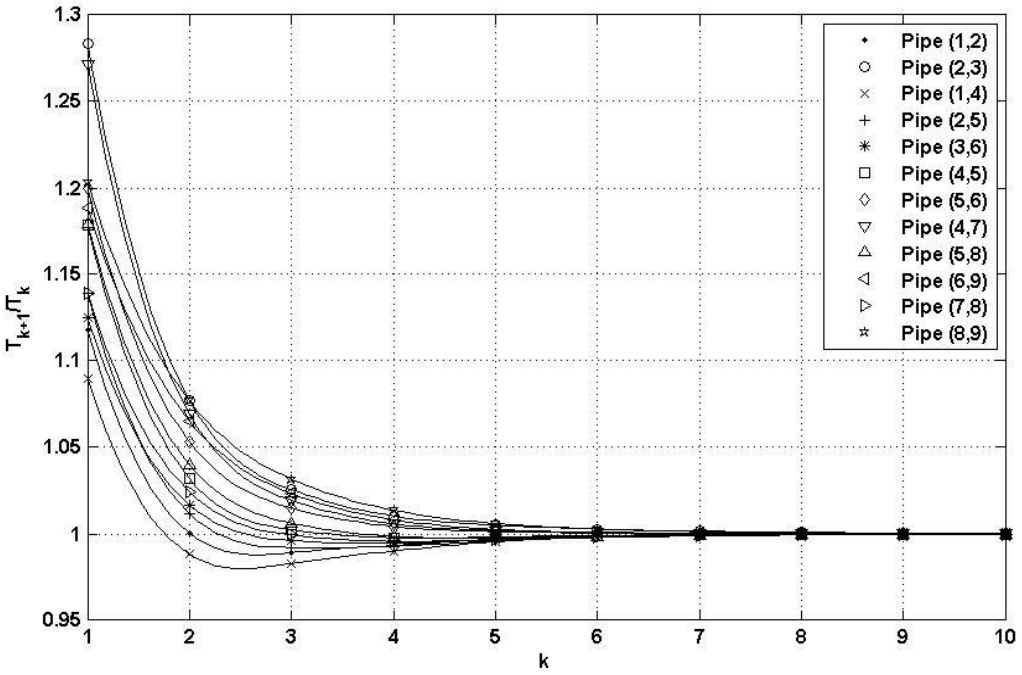

Figure 5.2.1: Analog pipe conductivity transform improvement ratio (T_{k+1}/T_k) vs. no. of iterations (k) – Case Study 2

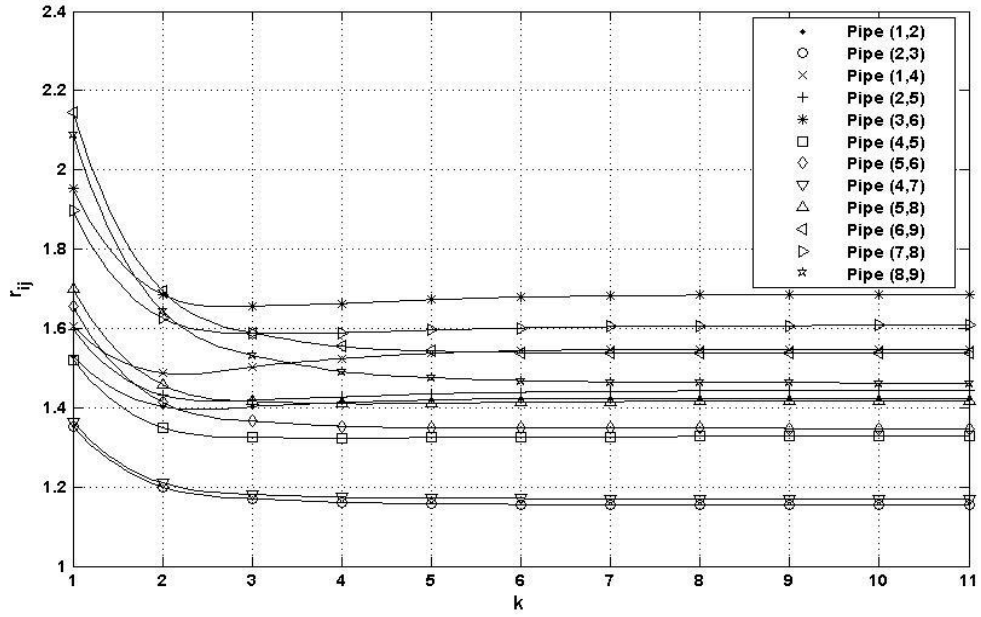

Figure 5.2.2: Pressure ratio (r_{ij}) vs. no. of iterations (k) – Case Study 2

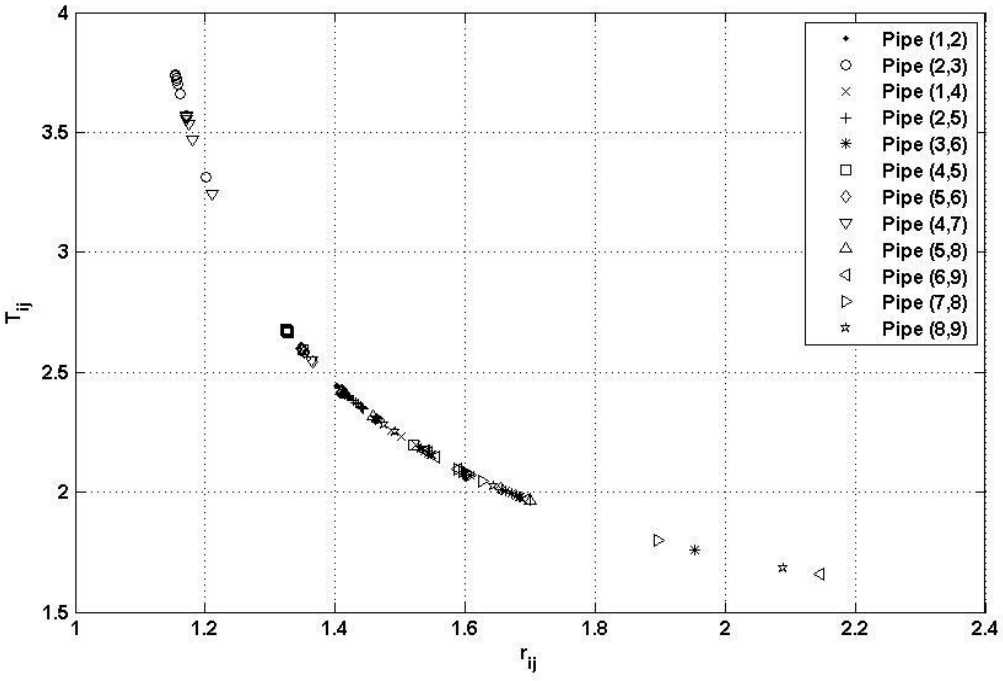

Figure 5.2.3: Analog conductivity transform (T_{ij}) vs. pressure ratio (r_{ij}) – Case Study 2

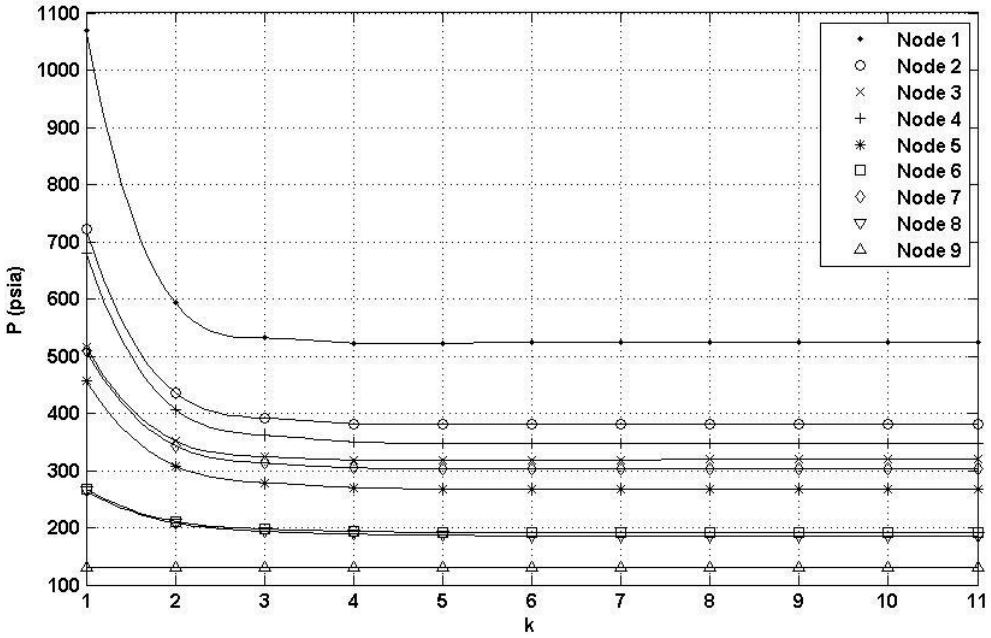

Figure 5.2.4: Nodal pressures (p_i) vs. no. of iterations (k) – Case Study 2

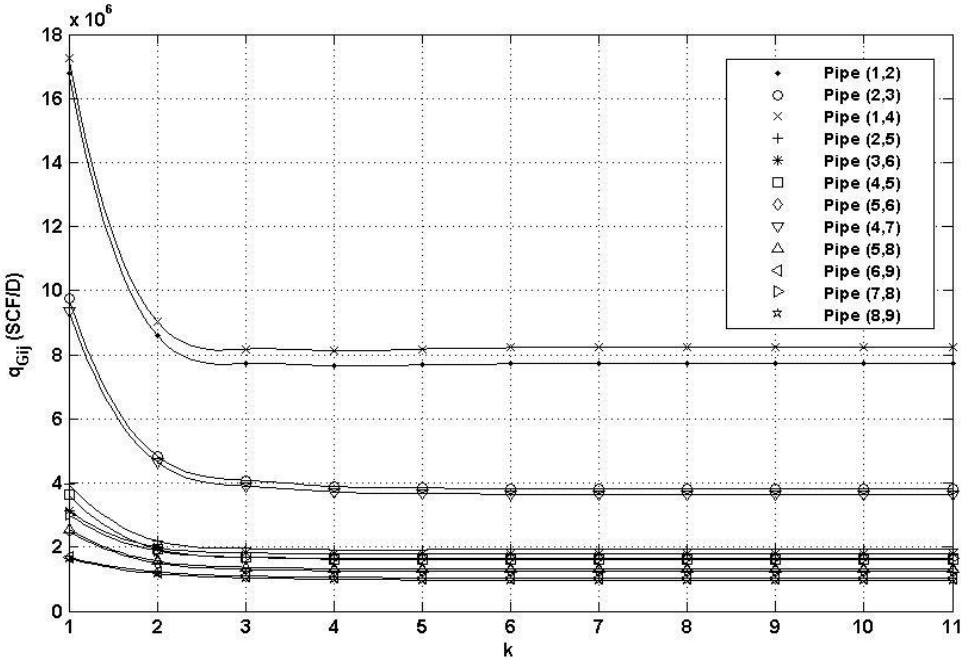

Figure 5.2.5: Pipe flow rate (q_{Gij}) vs. no. of iterations (k) – Case Study 2

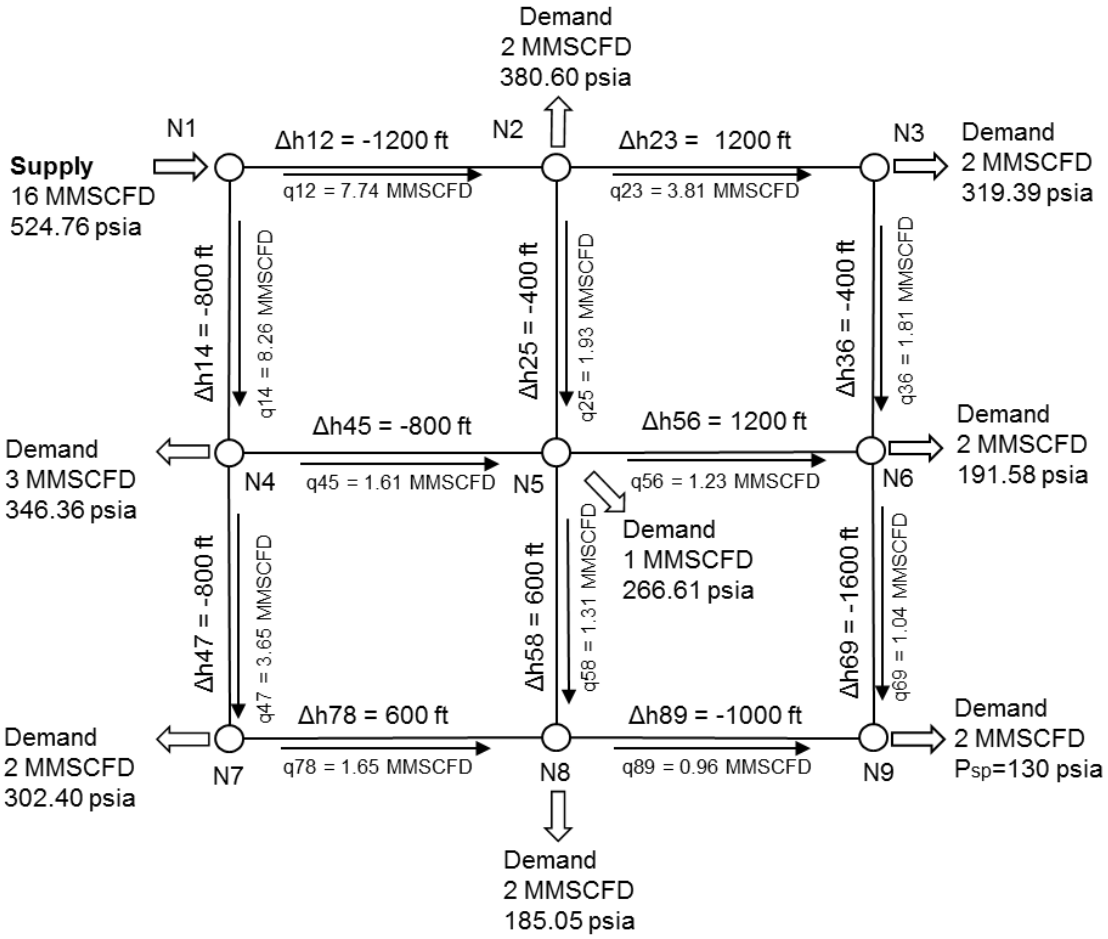

Figure 5.2.6: Fully-converged natural gas network distribution – Case Study 2

5.3 Case Study 3: Network System with Compression

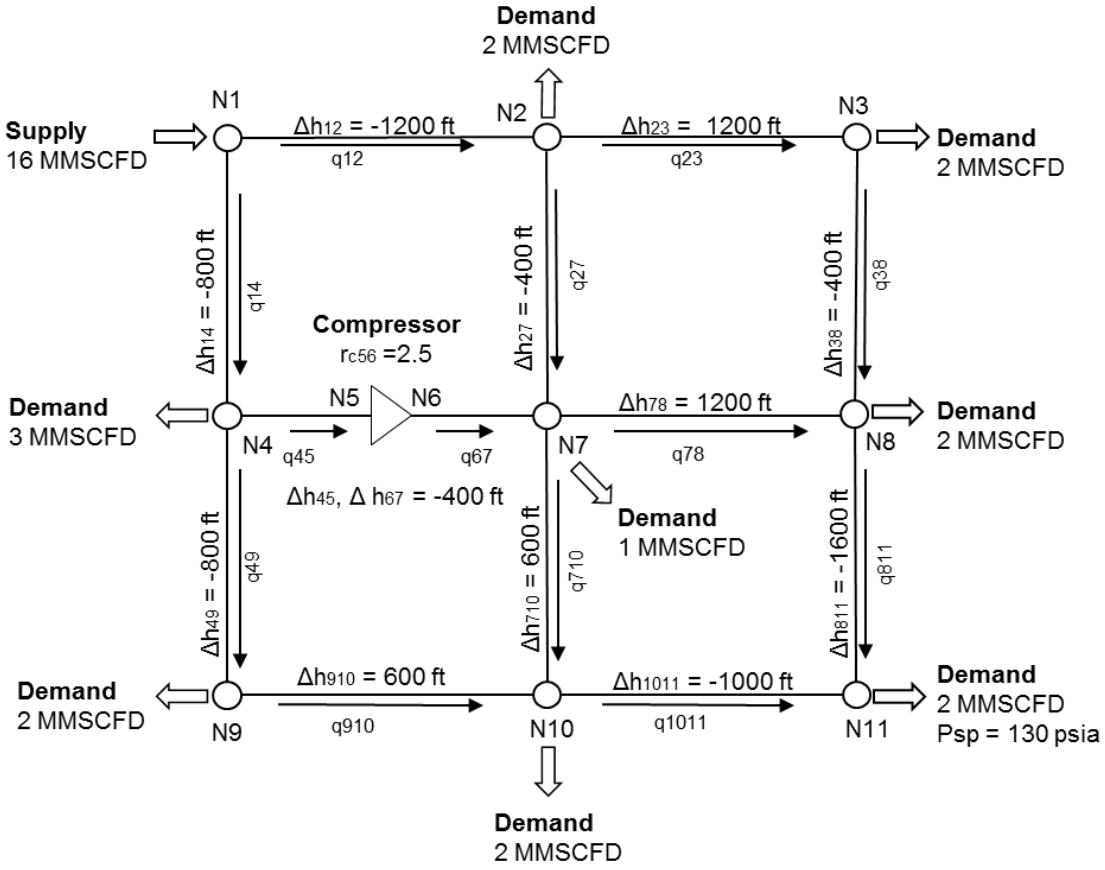

Figure 5.3: Network Topology of Case Study 3

Case Study 3 models an identical network with the elevated-mode scenario as the one presented in Case Study 2, but with an additional network component – a compressor. A compressor is located in between node 5 and node 6 and pipe (4,5) and pipe (6,7) are both 15 miles in length. The compressor is located at an elevation of 400 ft with respect to the datum at node 11. Suction temperature and average gas compressibility of gas at compressor are assumed to be 75 ℉ and 0.9, respectively, with a polytropic exponent of 1.4 and a compressor efficiency of 0.9. The compressor is operating at a target

compression ratio of 2.50 with a single stage (n_{st}=1). Node 11 is again specified at a pressure of 130 psia. This case study attempts to incorporate a compressor system into the linear-analog model, which was neglected in both the previous case studies. Similarly, based upon the implementation of the solution protocol in **Figure 4.3**, the application of the linear-pressure analog constitutive equations for elevated pipes in (4.9) coupled with a compressor equation in (4.19) to the gas network under study generates the following linear system of algebraic equations:

$$\begin{bmatrix} -O_1 & e^{s_{12}/2}L_{12} & 0 & e^{s_{14}/2}L_{14} & 0 & 0 & 0 & 0 & 0 & 0 & 0 \\ L_{12} & -O_2 & e^{s_{23}/2}L_{23} & 0 & 0 & 0 & e^{s_{27}/2}L_{27} & 0 & 0 & 0 & 0 \\ 0 & L_{23} & -O_3 & 0 & 0 & 0 & 0 & e^{s_{38}/2}L_{38} & 0 & 0 & 0 \\ L_{14} & 0 & 0 & -O_4 & e^{s_{45}/2}L_{45} & 0 & 0 & 0 & e^{s_{49}/2}L_{49} & 0 & 0 \\ 0 & 0 & 0 & L_{45} & -O_5 & -C_{C56} & 0 & 0 & 0 & 0 & 0 \\ 0 & 0 & 0 & 0 & -r_{56}L_{67} & -O_6 & e^{s_{67}/2}L_{67} & 0 & 0 & 0 & 0 \\ 0 & L_{27} & 0 & 0 & r_{56}L_{67} & 0 & -O_7 & e^{s_{78}/2}L_{78} & 0 & e^{s_{710}/2}L_{710} & 0 \\ 0 & 0 & L_{38} & 0 & 0 & 0 & L_{78} & -O_8 & 0 & 0 & e^{s_{811}/2}L_{811} \\ 0 & 0 & 0 & L_{49} & 0 & 0 & 0 & 0 & -O_9 & e^{s_{910}/2}L_{910} & 0 \\ 0 & 0 & 0 & 0 & 0 & 0 & L_{710} & 0 & L_{910} & -O_{10} & e^{s_{1011}/2}L_{1011} \\ 0 & 0 & 0 & 0 & 0 & 0 & 0 & 0 & 0 & 0 & 1 \end{bmatrix} \begin{bmatrix} p_1 \\ p_2 \\ p_3 \\ p_4 \\ p_5 \\ HP \\ p_7 \\ p_8 \\ p_9 \\ p_{10} \\ p_{11} \end{bmatrix} = \begin{bmatrix} -16 \\ 2 \\ 2 \\ 3 \\ 0 \\ 0 \\ 1 \\ 2 \\ 2 \\ 2 \\ 130 \end{bmatrix}$$

which, in compact notation, is expressed as:

$$\mathbf{K\,P = S}$$

In this particular case, the system of equations is constructed based upon the topology of the compressor. Note that the **P** network pressure vector is slightly different from the two previous case studies as the horsepower (HP) is represented here in node 6. The pressure of the downstream node of the compressor is substituted as the unknown since the pressure at node 6 is a function of the compression ratio given by $r_{c56} = \frac{P_6}{P_5}$. Hence the pressure at node 6 is expressed as the pressure of node 5 by equating $P_6 = r_{c56}.P_5$. The

network consumption/supply vector **S** is similar except that there are no consumption and supply at node 5 and 6. Characteristic matrix diagonal entries O_i are no longer just the summation of all off-diagonal entries where compressors are defined, for example, as it is at node 5 and node 6 in this case. Thus, $O_5 = e^{s_{45}/2}.L_{45}$ *; and* $O_6 = -C_{C56}$ are obtained according to the compressor location. In the upper right matrix, compressor constant, $-C_{C56,}$ is set to replace the pipe conductivity connecting node 5 and node 6 since it is connected by a compressor. In the lower left matrix where compressors are located, the pressures at node 6 is replaced with $P_6 = r_{c56}.P_5$. A negative sign is introduced at $\mathbf{K_{65}}$ **and** $\mathbf{K_{56}}$ because flow is leaving from the node 6. All pipes conductivities (L_{ij}) remain in MMSCFD/psi and the compressor constant (C_{Cij}) is in MMSCFD/HP in this example. The resulting characteristic matrix **K** remains banded but no longer symmetric; therefore the implementation of a Cholesky decomposition is no longer possible as it was for the previous case study 2. Therefore, the resulting system of linear equations could then be directly solved using any other standard linear equation solver such as LU decomposition, Gaussian Elimination, or Conjugate Gradient methods. **Figure 5.3.1 to 5.3.5** again present the results of such iterative solution protocol which follows the workflow of **Figure 4.3**. Final converged values or the actual network solution is displayed in **Figure 5.3.6**. The compressor horsepower is computed to be 149.60 HP. As previously shown, analog conductivity and pressure ratios steadily converge to true values (**Figure 5.3.1** and **5.3.2**, respectively) and maintain the same functional dependency among them (**Figure 5.3.3**). Pressure and flow rate estimations converge steadily and progressively as highlighted in **Figures 5.3.4 and 5.3.5**, respectively. Again, flow rates and pressures are

initially overestimated at the beginning because of the actual pipe conductivity is used in the linear-analog constitutive equation for the first iteration. Convergence behavior remains smooth and steady.

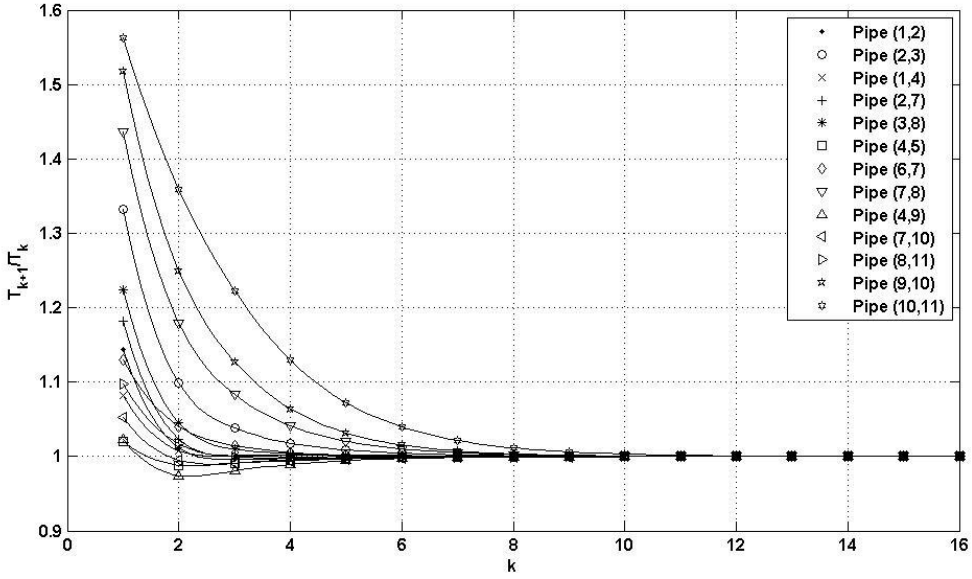

Figure 5.3.1: Analog conductivity transform improvement ratio (T_{k+1}/T_k) vs. no. of iterations (k) – Case Study 3

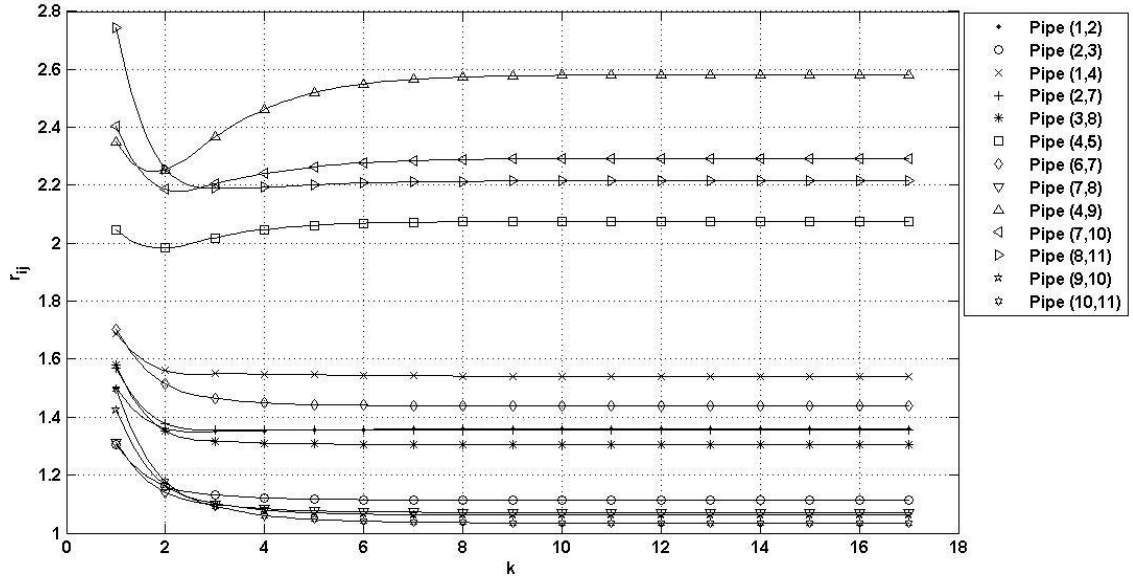

Figure 5.3.2: Pressure ratio (rij) vs. no. of iterations (k) – Case Study 3

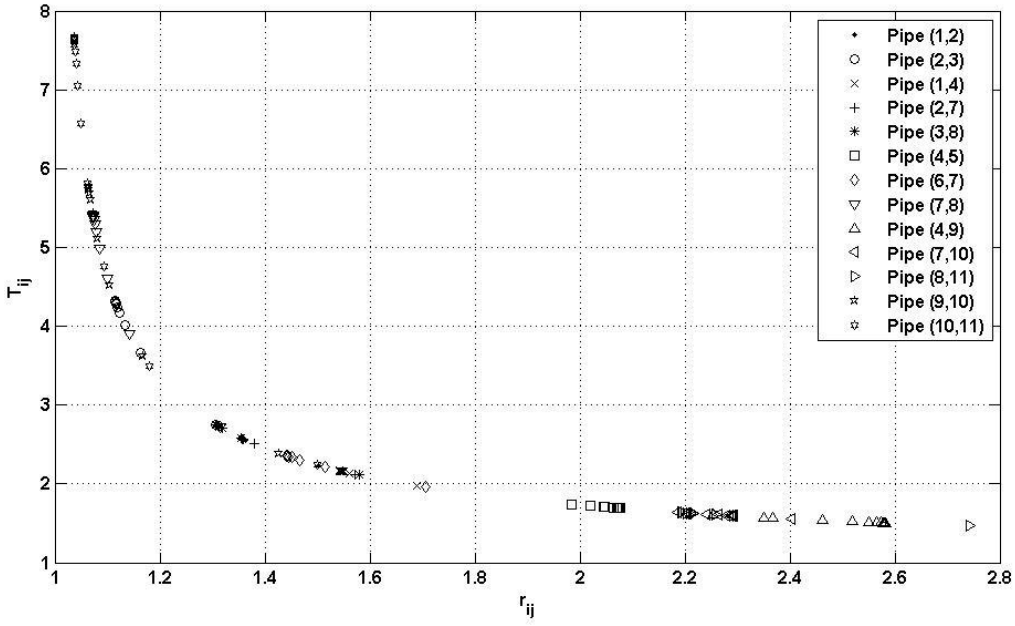

Figure 5.3.3: Analog conductivity transform (Tij) vs. pressure ratio (rij) – Case Study 3

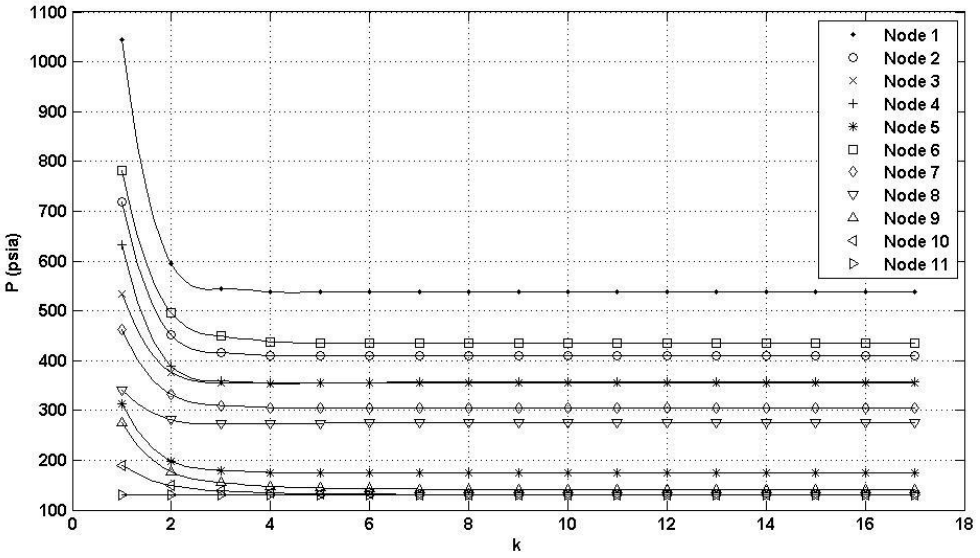

Figure 5.3.4: Nodal pressures (pi) vs. no. of iterations (k) – Case Study 3

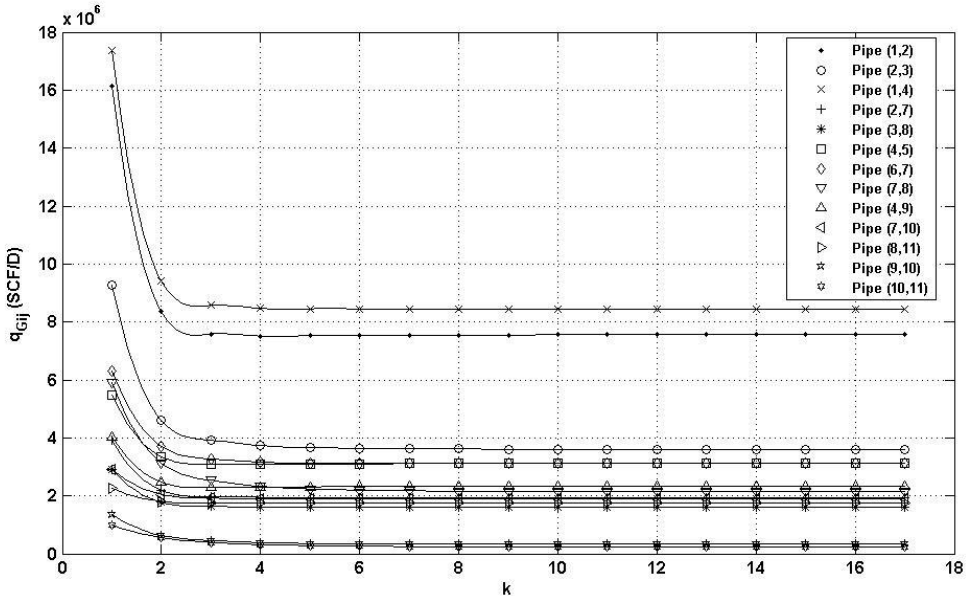

Figure 5.3.5: Pipe flow rate (qGij) vs. no. of iterations (k) – Case Study 3

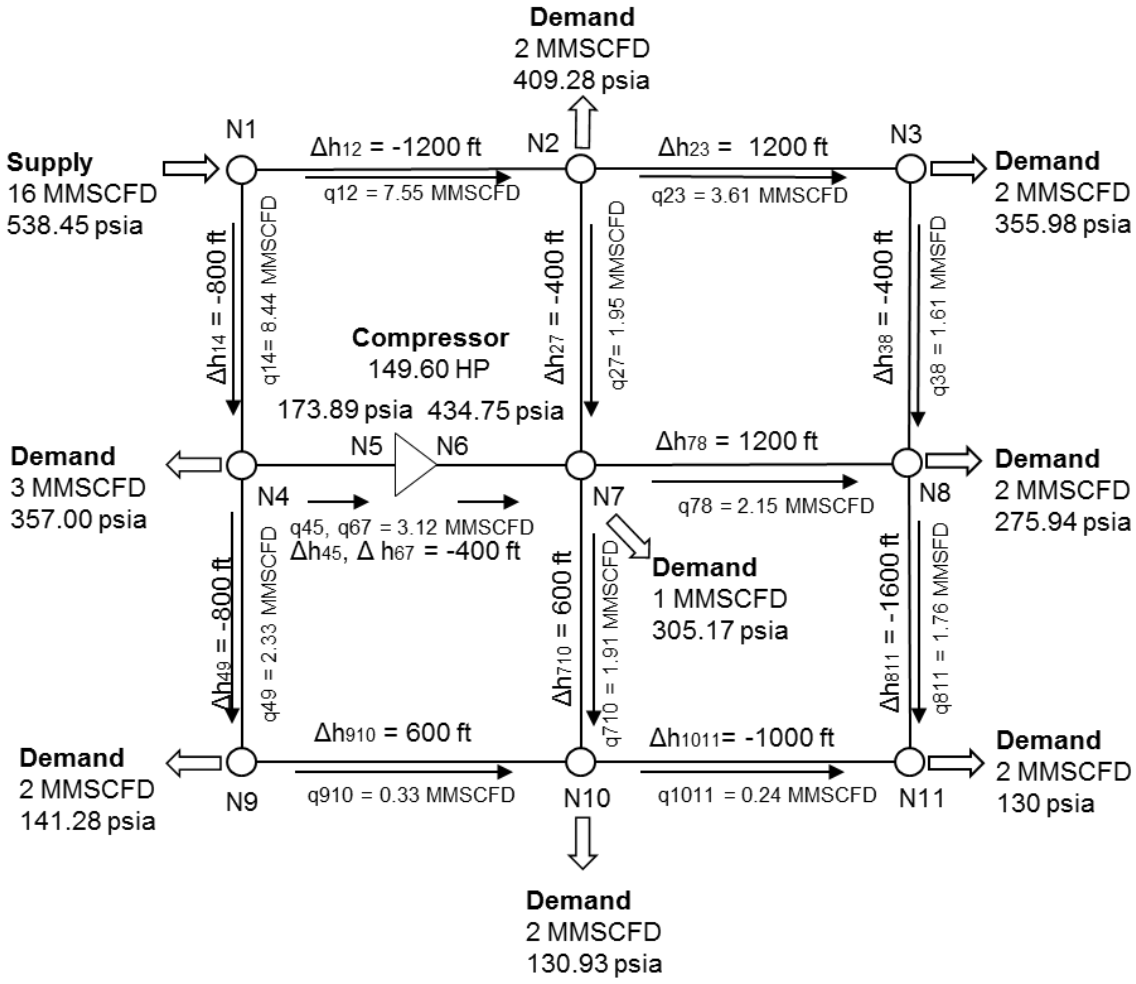

Figure 5.3.6: Fully-converged natural gas network distribution – Case Study 3

5.4 Case Study 4: Network System with Wellheads

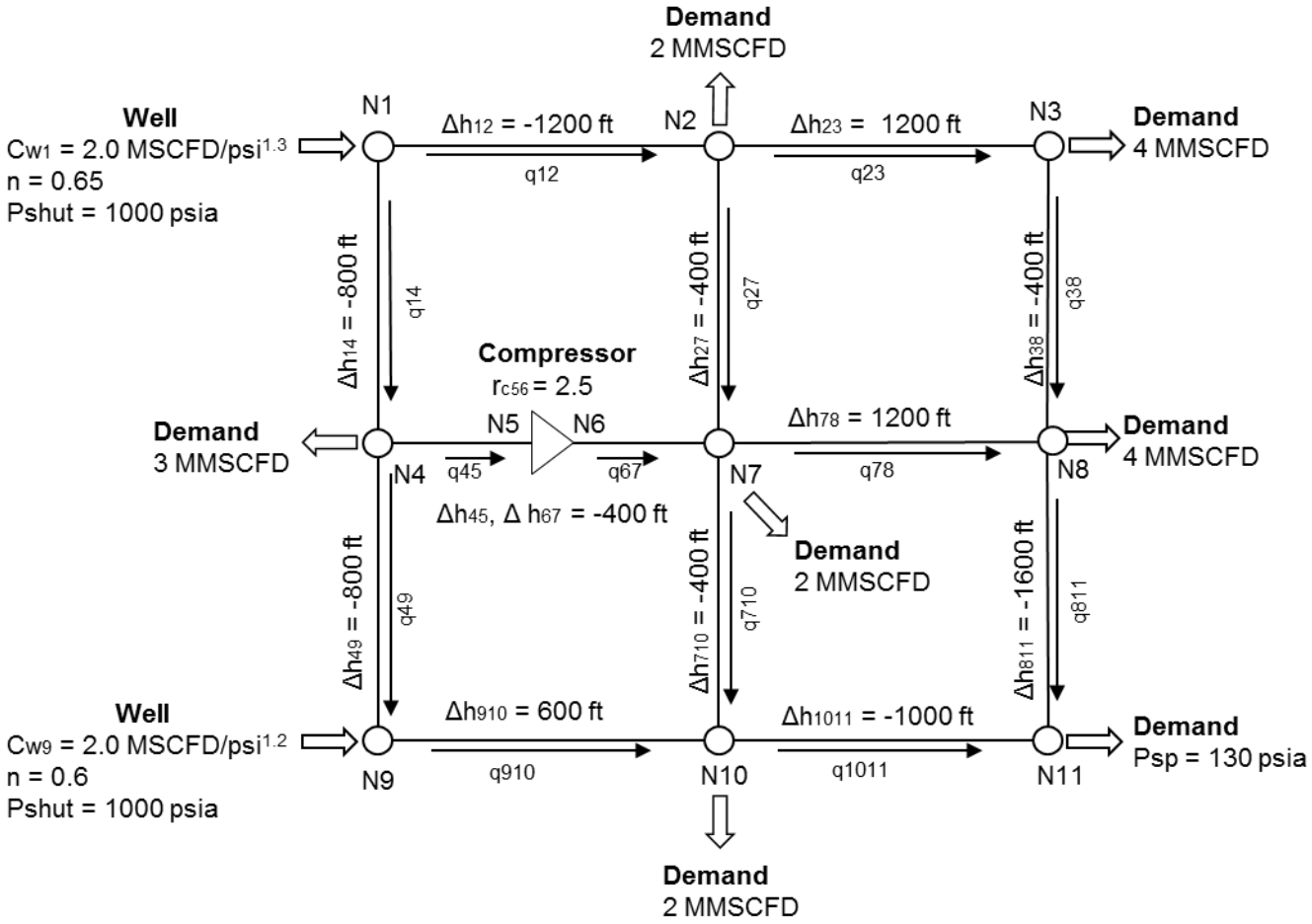

Figure 5.4: Network Topology of Case Study 4

Case Study 4 illustrates an identical network with the elevation scenario as presented in Case Study 2 and 3, but comprises additional network components – a compressor and wellheads. A compressor is again located between node 5 and node 6 and pipe (4,5) and pipe (6,7) are both 15 miles in length. Properties of gas flowing through the compressor are the same as for Case Study 2 and 3. The compressor is again operating at a given compression ratio of 2.5 with a single compression stage, with all other compression

parameters maintained the same. This case study ventures to encompass a compressor and wellheads system into the linear-analog model with a specified pressure of 130 psia at node 11. Demands are slightly higher at nodes 3, 7 and 8 compared to the previous cases to accommodate for the additional supply from the new wells. Demand at node 11 is set to be dependent on the specified pressure since the total supplies are a function of the wellhead pressures. Well 1 and Well 9 are assumed to have well conductivities C_{w1} of 2.0 MSCFD/psi$^{1.3}$, C_{w9} of 2.0 MMSCFD psi$^{1.2}$ and both of the wells are operating at a shut-in pressure of 1000 psia. The flow exponents are assumed to be 0.65 for the well at node 1 and 0.60 for the well at node 9. Utilizing the solution protocol in **Figure 4.3**, the application of the linear-pressure analog constitutive equation in (4.9) coupled with the compressor equation (4.19) and the wellheads equation in (4.22) to the gas network under study generates the following linear system of algebraic equations:

$$\begin{bmatrix}
-O_1 & e^{s_{12}/2}L_{12} & 0 & e^{s_{14}/2}L_{14} & 0 & 0 & 0 & 0 & 0 & 0 & 0 \\
L_{12} & -O_2 & e^{s_{23}/2}L_{23} & 0 & 0 & 0 & e^{s_{27}/2}L_{27} & 0 & 0 & 0 & 0 \\
0 & L_{23} & -O_3 & 0 & 0 & 0 & 0 & e^{s_{38}/2}L_{38} & 0 & 0 & 0 \\
L_{14} & 0 & 0 & -O_4 & e^{s_{45}/2}L_{45} & 0 & 0 & 0 & e^{s_{49}/2}L_{49} & 0 & 0 \\
0 & 0 & 0 & L_{45} & -O_5 & -C_{C56} & 0 & 0 & 0 & 0 & 0 \\
0 & 0 & 0 & 0 & -r_{56}L_{67} & -O_6 & e^{s_{67}/2}L_{67} & 0 & 0 & 0 & 0 \\
0 & L_{27} & 0 & 0 & r_{56}L_{67} & 0 & -O_7 & e^{s_{78}/2}L_{78} & 0 & e^{s_{710}/2}L_{710} & 0 \\
0 & 0 & L_{38} & 0 & 0 & 0 & L_{78} & -O_8 & 0 & 0 & e^{s_{811}/2}L_{811} \\
0 & 0 & 0 & L_{49} & 0 & 0 & 0 & 0 & -O_9 & e^{s_{910}/2}L_{910} & 0 \\
0 & 0 & 0 & 0 & 0 & 0 & L_{710} & 0 & L_{910} & -O_{10} & e^{s_{1011}/2}L_{1011} \\
0 & 0 & 0 & 0 & 0 & 0 & 0 & 0 & 0 & 0 & 1
\end{bmatrix}
\begin{bmatrix} p_1 \\ p_2 \\ p_3 \\ p_4 \\ p_5 \\ HP \\ p_7 \\ p_8 \\ p_9 \\ p_{10} \\ p_{11} \end{bmatrix}
=
\begin{bmatrix} -P_{shut}.L_{w1} \\ 2 \\ 2 \\ 3 \\ 0 \\ 0 \\ 1 \\ 2 \\ -P_{shut}.L_{w9} \\ 2 \\ 130 \end{bmatrix}$$

which, in compact notation, is expressed as:

$$\mathbf{K\,P = S}$$

The system of equations is formulated based upon the topology of both the compressor and wellheads locations. Note that the **P** network pressure vector has the horsepower (HP) represented here in node 6. Similarly, the pressure of the downstream node of the compressor is substituted as the unknown since the pressure at node 6 is a function of the compression ratio given by $r_{56} = \frac{p_6}{p_5}$. Hence pressure at node 6 is expressed as the pressure of node 5 by equating $p_6 = r_{56}.p_5$. For the network consumption/supply vector **S,** besides that there are no consumption and supply at node 5 and 6, node 1 and node 9 are essentially producing as a function of the wells shut-in pressure since it is given by – $L_{wi}.p_{shut}$. Characteristic matrix diagonal entries O_i are not just the summation of all off-diagonal entries for where compressors are defined (For example, it is at node 5 and node 6 in this case). Thus, $O_5 = L_{45}$*; and* $O_6 = -C_{C56}$ are obtained. In the upper right matrix, the compressor constant $-C_{C56}$ is set to replace the pipe conductivity connecting node 5 and node 6 since it is connected by the compressor. In the lower left matrix where compressors are located, pressures at node 6 is replaced with $P_6 = r_{56}.P_5$. A negative sign is introduced at $\mathbf{K_{65}}$ **and** $\mathbf{K_{56}}$ because flow is leaving from the node 6. For the nodes with wells, changes are done on the vector **S** where the known shut-in pressures p_{shut} are moved to the residual vectors while the L_w are incorporated in the diagonal entries in characteristic matrix **K**. For instance, $O_1 = L_{12}+L_{14}+L_{w1}$ and $O_9 = L_{49}+L_{910}+L_{w9}$. All pipe conductivities (L_w, L_{ij}) remain in MMSCFD/psi^{2n} and the compressor constant (C_{Cij}) is in MMSCFD/HP in this example. Likewise, the resulting characteristic matrix **K** remains banded but no longer symmetric; therefore, the implementation of Cholesky

decomposition is no longer possible as it was for the previous case studies. Therefore, the resulting system of linear equations could then be directly solved using any other standard linear equation solver such as LU decomposition, Gaussian Elimination, or Conjugate Gradient methods. **Figure 5.4.1 to 5.4.5** establishes the results of such iterative solution protocol which follows the workflow of **Figure 4.3**. Final converged values or the actual network solution is displayed in **Figure 5.4.6**. The compressor is determined to be operating at a horsepower of 201.81 HP and Well 1 and Well 9 are producing at 13.07 MMSCFD and 6.16 MMSCFD, respectively. Note that the flow rates for pipe (4,9) and pipe (7,10) are actually flowing the opposite direction from the initial flow direction. This could be seen in the initial underestimated pressure ratios in **Figure 5.4.2**. As previously shown, analog conductivity and pressure ratios steadily converge to true values (**Figure 5.4.1** and **5.4.2**, respectively) and maintain the same functional dependency among them (**Figure 5.4.3**). Pressure and flow rate estimations converge steadily and progresively as highlighted in **Figures 5.4.4 and 5.4.5**, respectively. Convergence behavior remains smooth and steady.

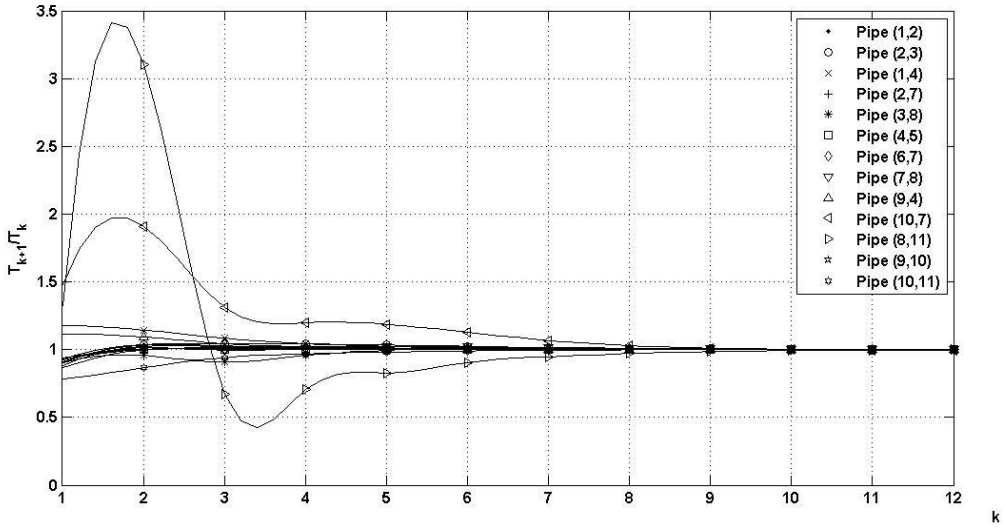

Figure 5.4.3: Analog conductivity transform improvement ratio (T_{k+1}/T_k) vs. no. of iterations (k) – Case Study 4

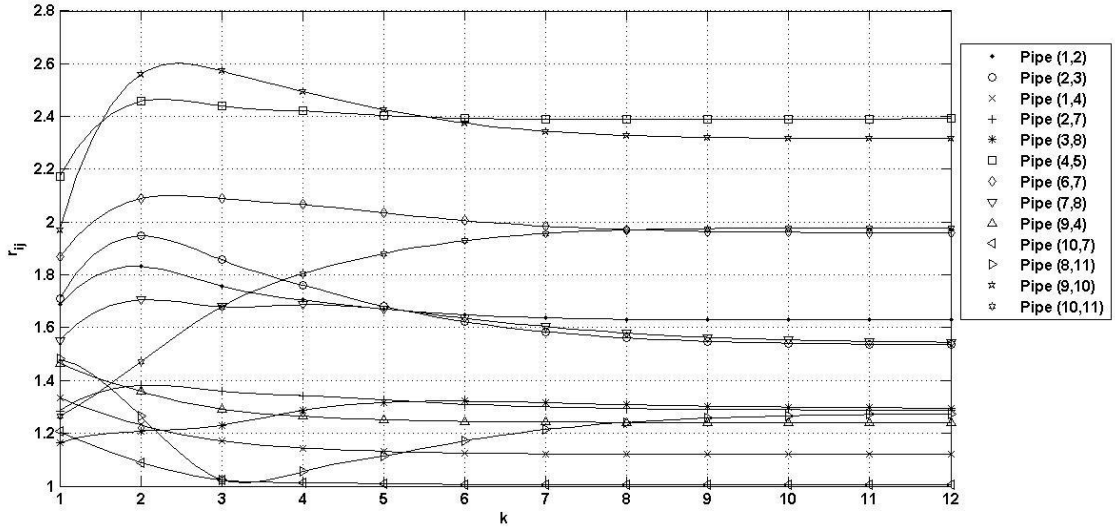

Figure 5.4.4: Pressure ratio (rij) vs. no. of iterations (k) – Case Study 4

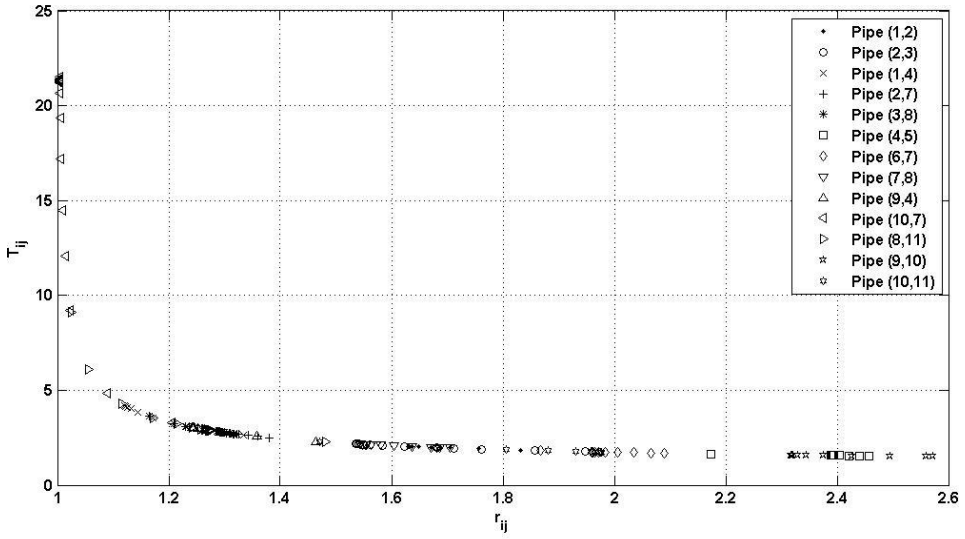

Figure 5.4.5: Analog conductivity transform (T_{ij}) vs. pressure ratio (r_{ij}) – Case Study 4

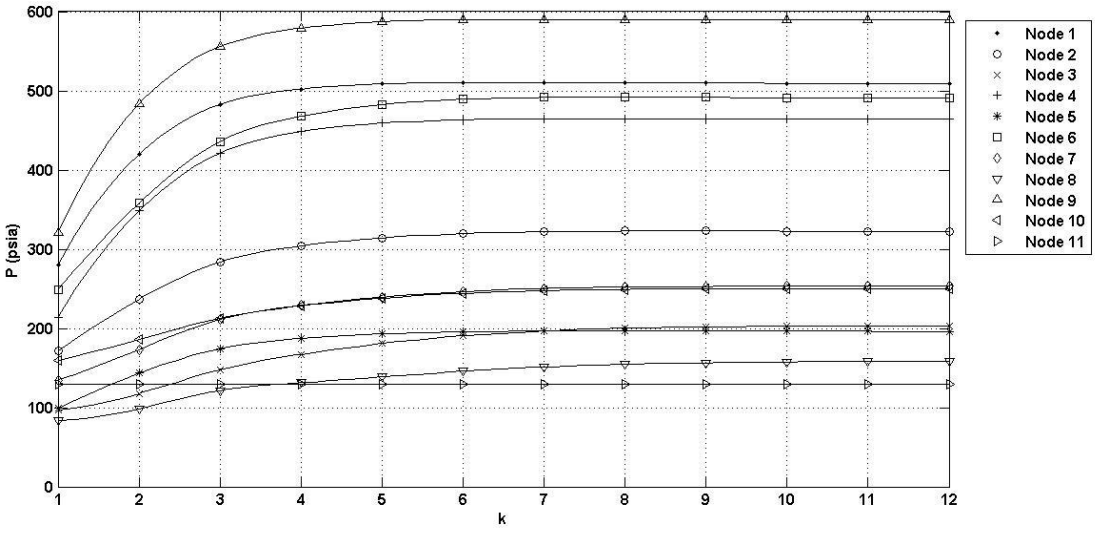

Figure 5.4.4: Nodal pressures (p_i) vs. no. of iterations (k) – Case Study 4

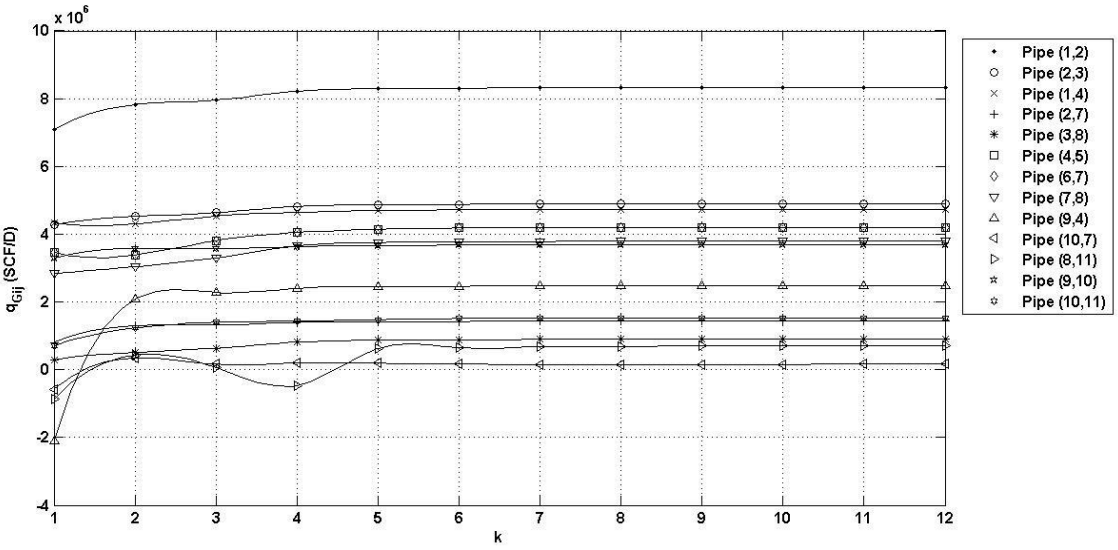

Figure 5.6.5: Pipe flow rate (q_{Gij}) vs. no. of iterations (k) – Case Study 4

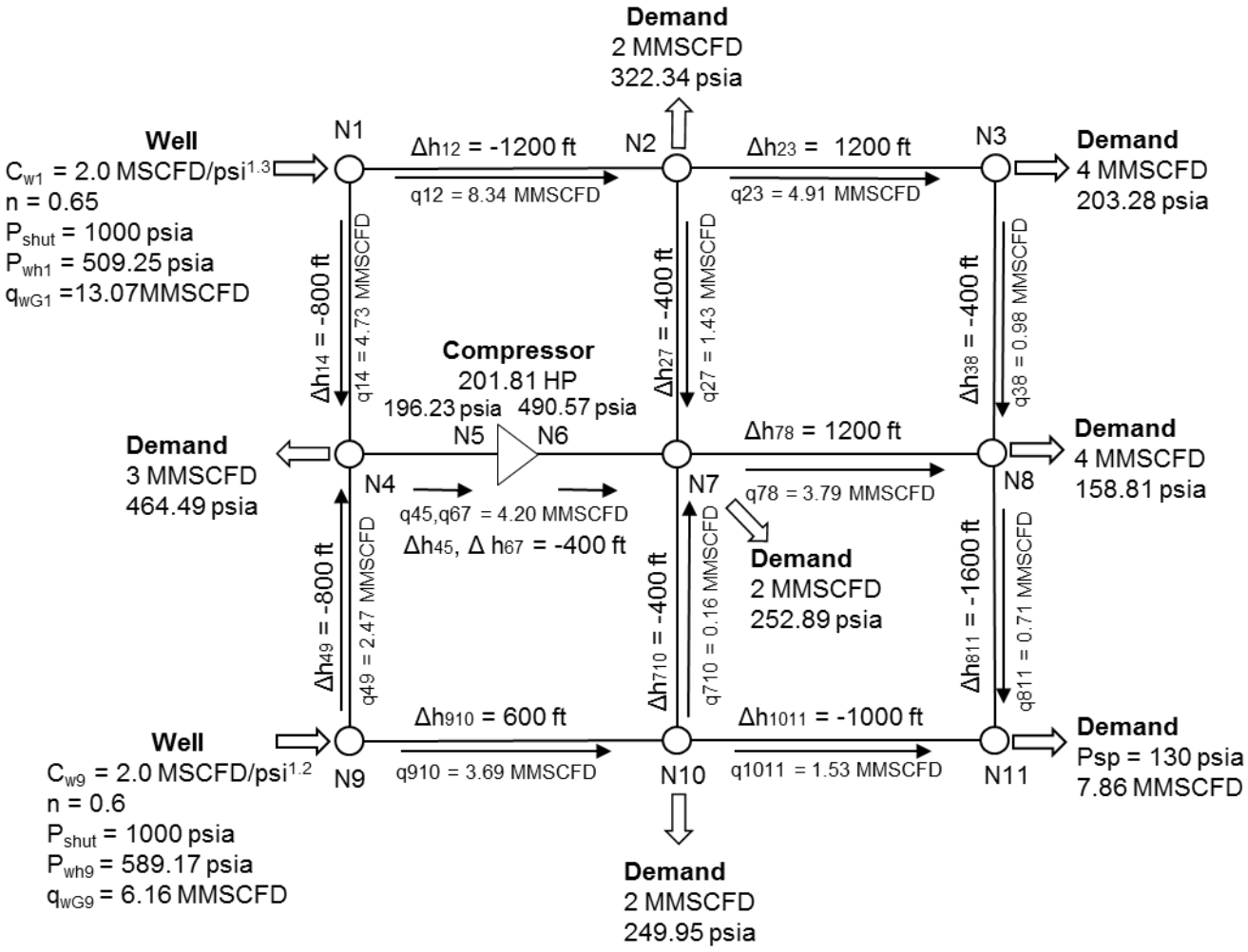

Figure 5.4.6: Fully-converged natural gas network distribution – Case Study 4

5.5 Case Study 5: Mexico Valley Field Case

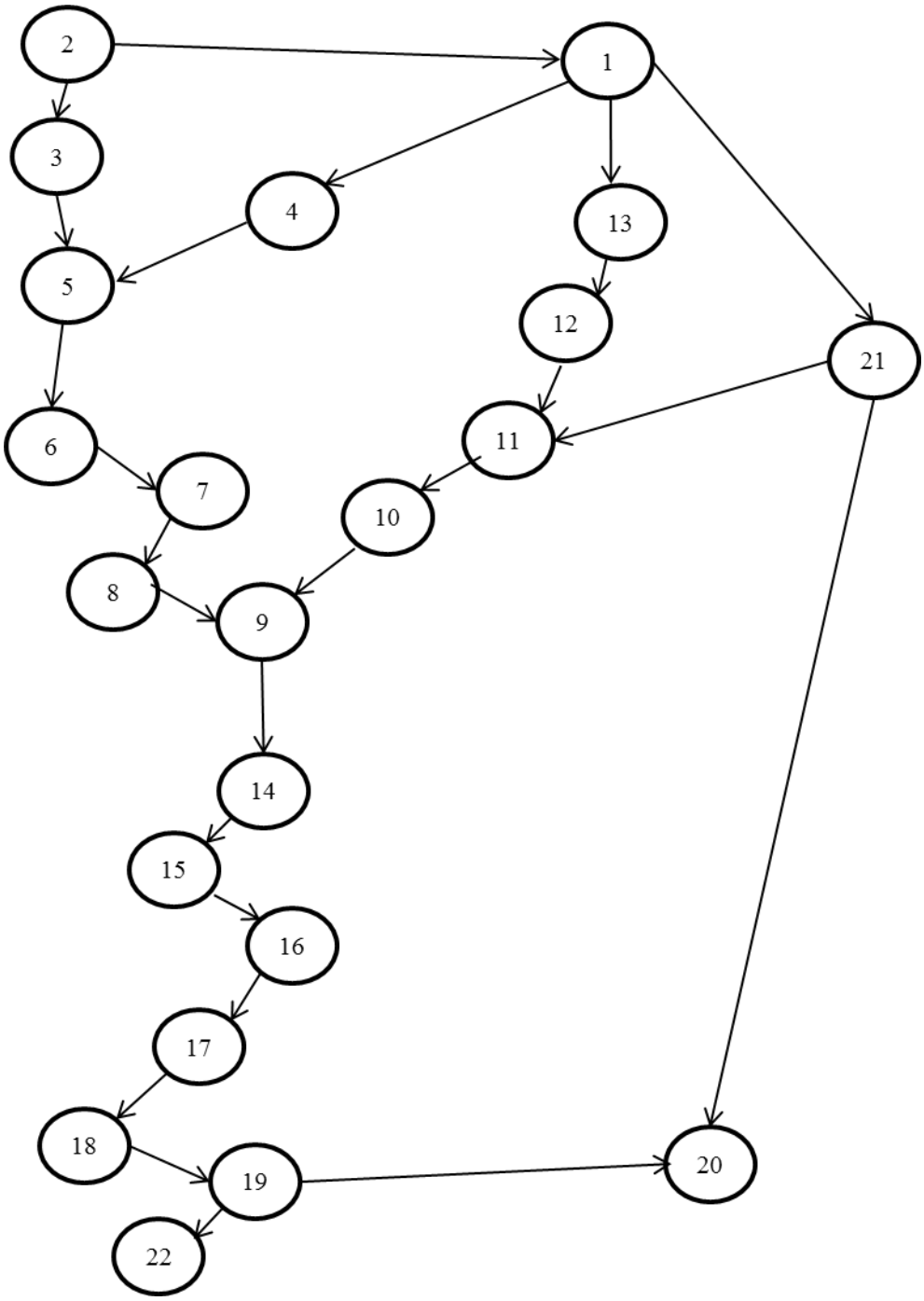

Figure 5.5 Network Topology of Mexico Valley

Case Study 5 evaluates a real gas distribution grid in the Mexico Valley (Nagoo, 2003; Martinez-Romero, Osorio-P, and Santamaria-V., 2002; Montoya-O., Jovel-T., Hernandez-R, and Gonzalez-R, 2000). The grid connects twenty-two cities, which is illustrated in **Figure 5.5**. There are twenty-five pipes connecting these city stations and properties of these pipes are given in **Table 5.5.1** below. Elevation changes are deemed unimportant by the original study and natural gas is said to be supplied at Venta de Carpio with an inlet pressure of 350 psia, with a gas specific gravity of 0.65, and an average flow temperature of 345 ℜ. Pipes are assumed to be operating at an efficiency of 0.80 with an average gas compressibility of 0.98. The model is run on the basis of the Panhandle-B gas flow equation. Pipe properties are summarized in **Table 5.5.1** while supplies and demand are given on the **Table 5.5.2** later.

Table 5.5.1: Pipe Network Properties for Case Study 5

Input node	Output node	Length (m)	Length (miles)	Diameter (in)
1	2	21375.50	13.28	12
1	4	23688.90	14.72	20
1	13	5101.48	3.17	22
1	21	14789.47	9.19	24
2	3	3749.67	2.33	14
3	5	1577.11	0.98	14
4	5	1699.42	1.06	20

5	6	3170.32	1.97	14
6	7	1309.97	0.81	14
7	8	3556.55	2.21	20
8	9	1995.53	1.24	20
9	10	7740.73	4.81	22
9	14	788.56	0.49	22
10	11	7724.64	4.79	22
11	12	1947.25	1.21	22
11	21	2494.42	1.55	20
12	13	3685.30	2.29	22
14	15	4441.67	2.76	12
15	16	2124.28	1.32	22
16	17	2285.21	1.42	14
17	18	1995.53	1.24	14
18	19	8191.34	5.09	14
19	20	24413.08	15.17	10
19	22	2478.32	1.54	3
21	20	31461.82	19.55	14

Figures 5.5.1 to 5.5.5 below again exhibit the results of the iterative solution protocol as followed in the workflow of **Figure 4.3**. As previously shown, analog conductivity and pressure ratios steadily converge to true values (**Figure 5.5.1** and **5.5.2**, respectively) and

maintain the same functional dependency among them (**Figure 5.5.3**). Pressure and flow rate estimations converge steadily and progressively as highlighted in **Figures 5.5.4 and 5.5.5**, respectively. As seen in **Figure 5.5.4**, because the highest pressure in the system is specified, the initial pressures are underestimated. Convergence behavior however, remains smooth and steady as the number of iterations increases. Final converged values of the Mexico Valley network are summarized in **Table 5.5.2** below, which compare quite favorably against the reported pressure data by Martinez-Romero *et al.* (2002) with maximum deviation errors around 1%.

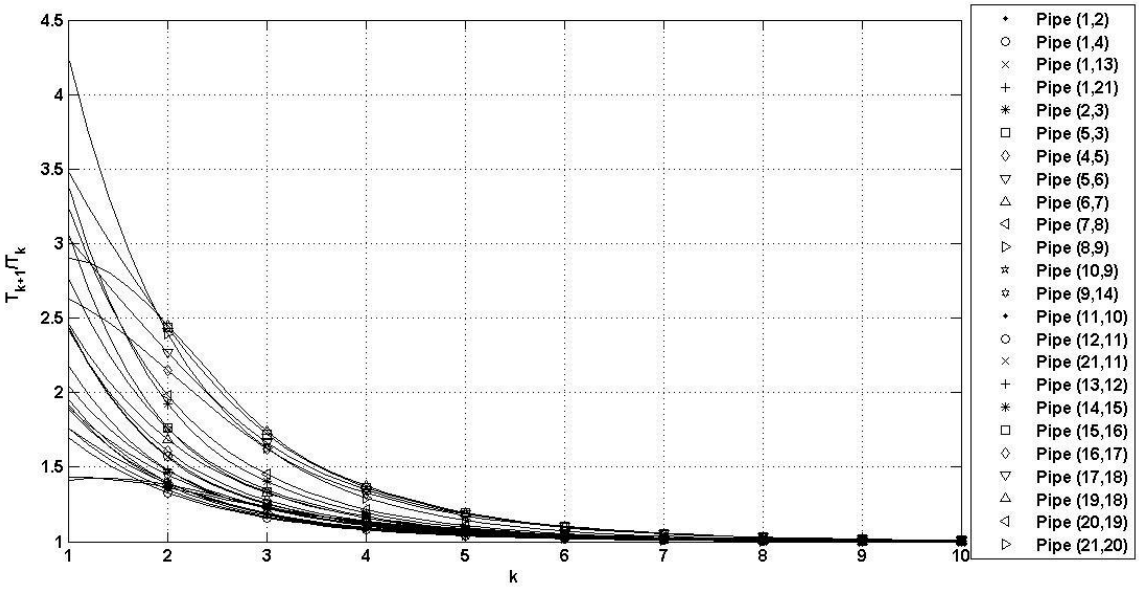

Figure 5.5.1: Analog conductivity transform improvement ratio (T_{k+1}/T_k) vs. no. of iterations (k) – Case Study 5

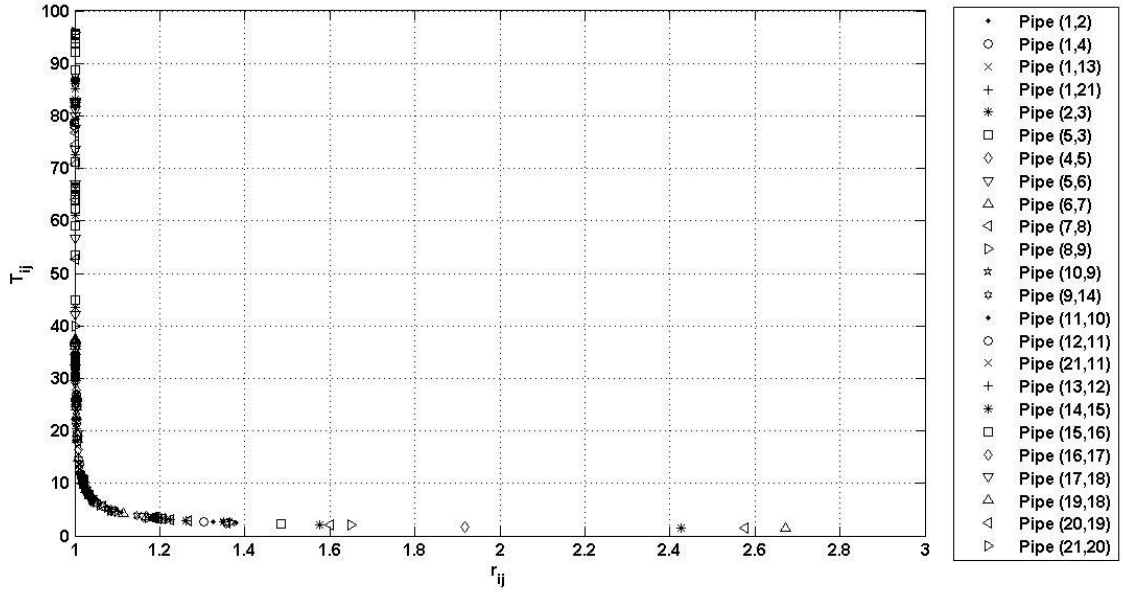

Figure 5.5.7: Pressure ratio (rij) vs. no. of iterations (k) – Case Study 5

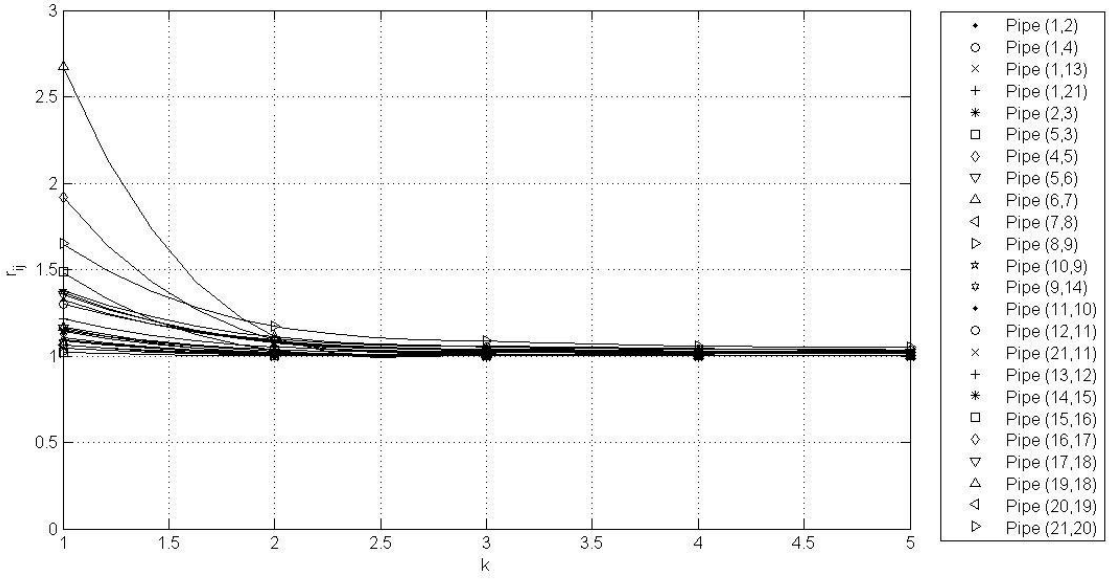

Figure 5.5.8: Analog conductivity transform (T_{ij}) vs. pressure ratio (r_{ij}) – Case Study 5

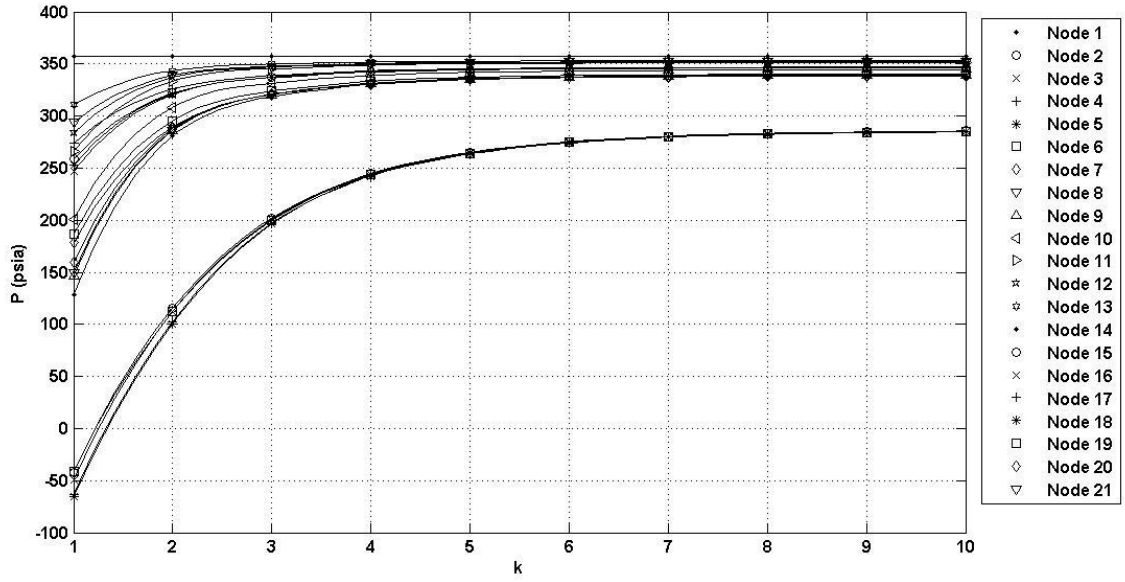

Figure 5.5.4: Nodal pressures (p_i) vs. no. of iterations (k) – Case Study 5

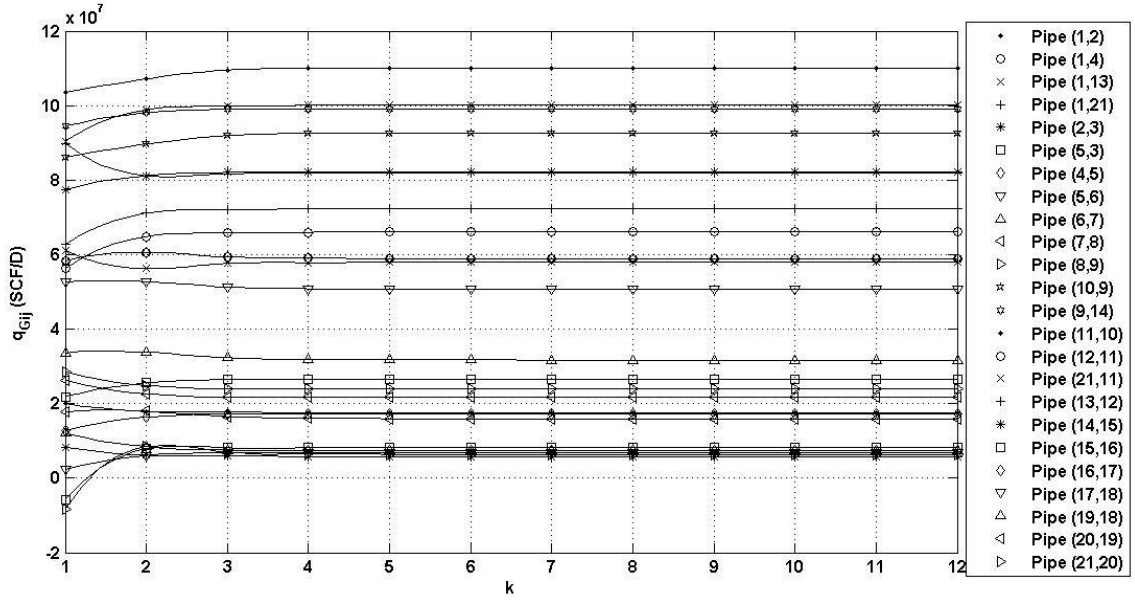

Figure 5.5.5: Pipe flow rate (q_{Gij}) vs. no. of iterations (k) – Case Study 5

Table 5.5.2: Nodal Network Predictions for Case Study 5

City	Node	Supply (-) / Demand (+) (MMSCFD)	Pressure reported by Martinez-Romero *et al.* (psia)	Calculated Pressure using Linear Analog Model (psia)	Deviation Error (%)
Venta de Carpio	1	-258.58	356.94	356.94	0.00%
Tultitlán	2	11.79	345.77	346.33	0.16%
Lechería	3	14.04	345.77	346.24	0.14%
Yets	4	0.00	346.49	347.00	0.15%
Barrientos	5	0.00	345.77	346.31	0.16%
Anahuac	6	18.96	340.26	340.42	0.05%
Romana	7	15.79	339.39	339.48	0.03%
Comunidad	8	9.58	339.24	339.37	0.04%
Río de los	9	0.00	339.24	339.36	0.03%
San Juanico	10	17.46	344.32	344.36	0.01%
Cerro Gordo	11	13.92	351.28	351.28	0.00%
Tulpetlac	12	6.29	351.86	351.88	0.01%
Sosa Texcoco	13	27.75	353.31	353.27	-0.01%
Vallejo	14	16.92	338.66	338.80	0.04%
18 de Marzo	15	55.63	289.49	286.58	-1.01%
Camarones	16	9.17	289.35	286.45	-1.00%
Anahuac 78	17	10.33	288.77	285.86	-1.01%
Anahuac 80	18	14.46	288.63	285.77	-0.99%

San Pedro de los Pinos	19	14.25	288.92	286.18	-0.95%
Coapa	20	2.25	338.66	338.61	-0.01%
Pinter	21	0.00	352.15	352.24	0.03%
Belén de las Flores	22	0.00	288.92	286.18	-0.95%

It is interesting to note that the initial pressures calculated by the linear-analog model are found to be negative in the first iteration (see **Figure 5.5.4**). This is to be expected because the specified nodal pressure for this case was prescribed upstream at the supply node. For such cases, and because of the assumption $L_{ij} = C_{ij}$ used in the first iteration, the linear-analog model overestimated pressure drops, thus yielding downstream negative pressures. Note that this behavior is possible because linear-analog conductivities used in the beginning of the iteration were deliberatively underestimated, thus making the system less conductive than it actually is. As previously discussed, one alternative way of circumventing this behavior is to initialize the system using higher linear conductivities; *i.e.*, using a multiple of the actual pipe conductivity ($L_{ij} = 2C_{ij}$, or $L_{ij} = 3C_{ij}$, for instance) instead of $L_{ij} = C_{ij}$ for initialization of linear conductivities in the first iteration. For this field scenario, for example, using an initialization $L_{ij} = 2C_{ij}$ eliminates all negative pressures originally found in the first iteration. The resulting graphs are generated below. **Figure 5.5.6 to Figure 5.5.8** show the convergence behavior of the linear-analog method when the initialization uses $L_{ij} = 2C_{ij}$. As it is seen in **Figure 5.5.9**, the initial calculated

pressures do no longer reach negative values and the convergence behavior remains quite stable and even improved. The pressures are calculated based on a higher analog conductivity and hence predict higher downstream pressure values earlier on. **Figure 5.5.10** shows the steady convergence of flow rate predictions for each pipe.

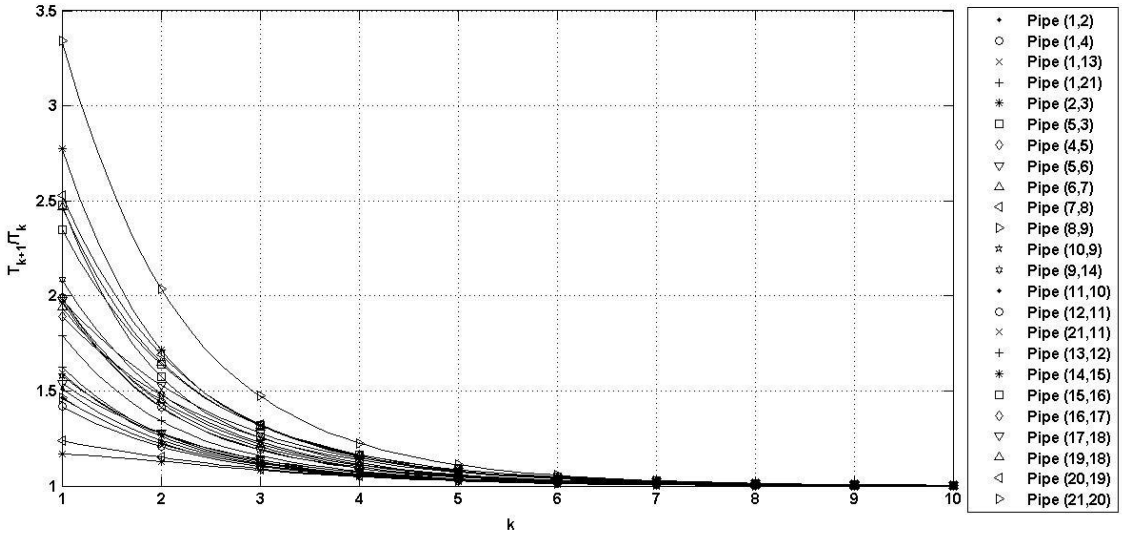

Figure 5.5.6: Analog conductivity transform improvement ratio (T_{k+1}/T_k) vs. no. of iterations (k) – Case Study 5

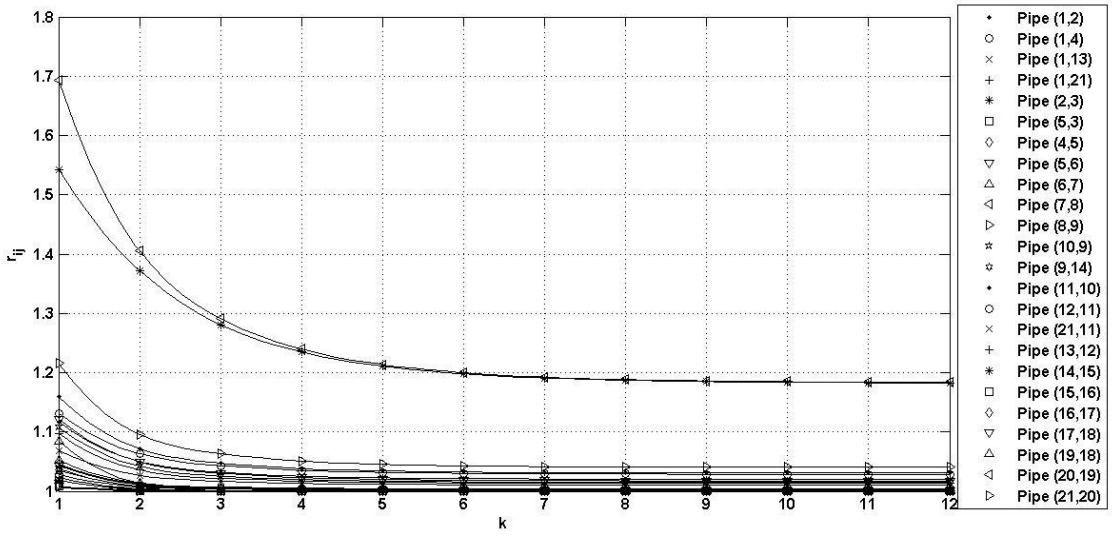

Figure 5.5.7: Pressure ratio (rij) vs. no. of iterations (k) – Case Study 5

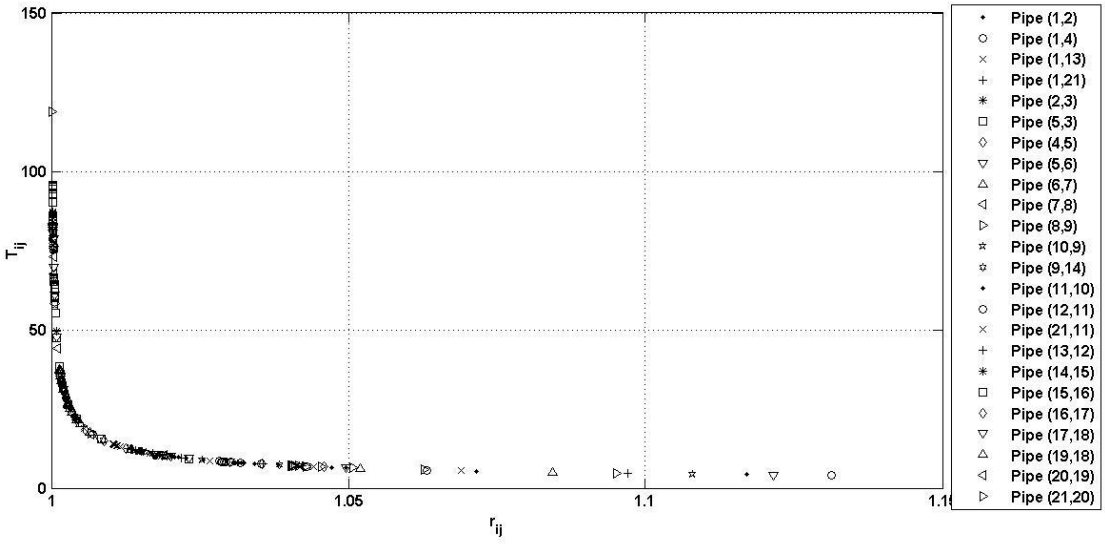

Figure 5.5.8: Analog conductivity transform (T_{ij}) vs. pressure ratio (r_{ij}) – Case Study 5

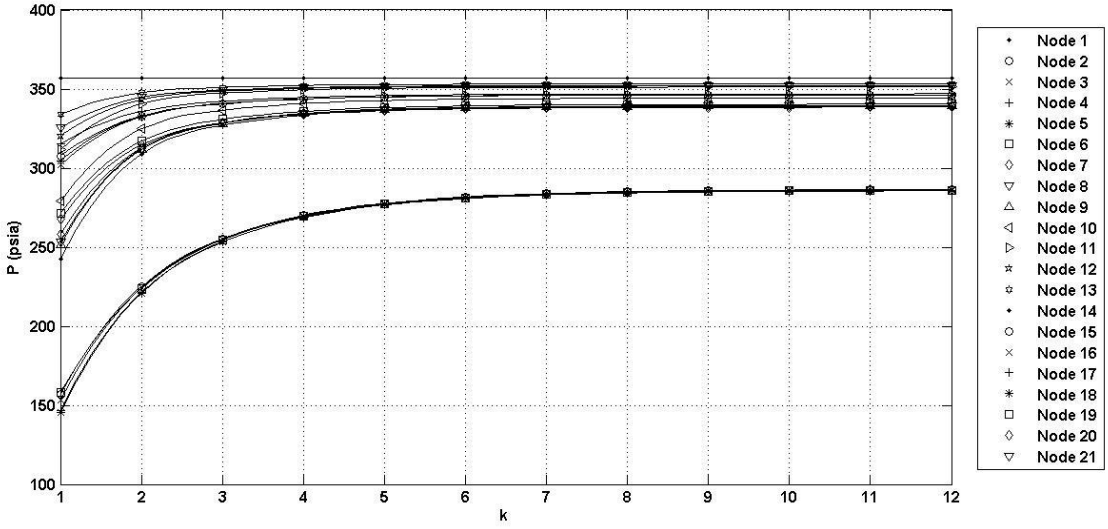

Figure 5.5.9: Nodal pressures (p_i) vs. no. of iterations (k) – Case Study 5

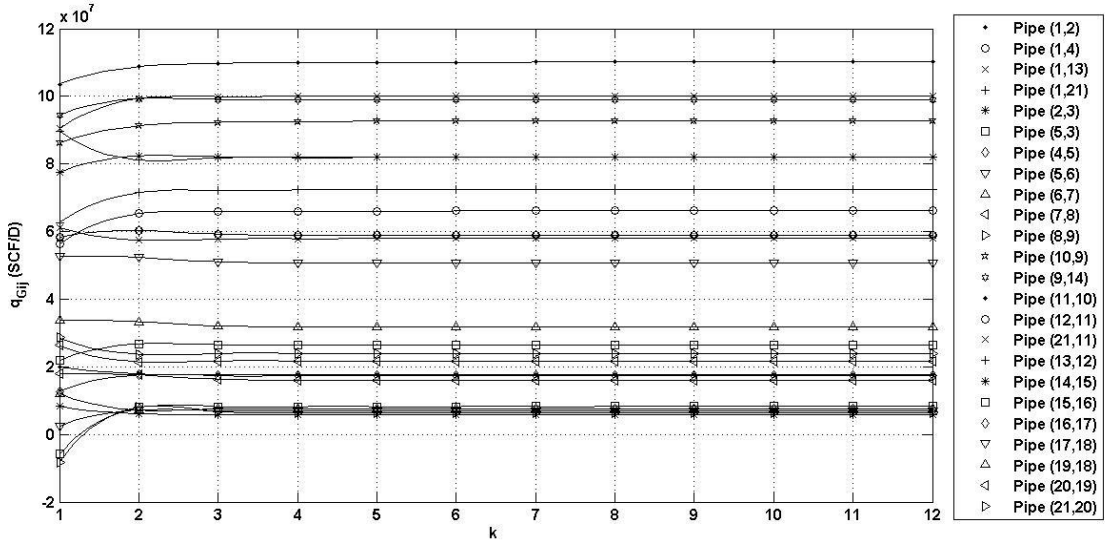

Figure 5.5.10: Pipe flow rate (q_{Gij}) vs. no. of iterations (k) – Case Study 5

CHAPTER 6

CONCLUDING REMARKS

A linear-pressure analog has been proposed for the solution of the highly non-linear equations typical of natural gas network transportation modeling. The approach does not need any type of initial guesses or user-provided pressure or flow rate initializations, as opposed to current standard practice that heavily relies on the application of Newton-Raphson-based protocols. The iterative method relies on the solution of successive interim, well-posed liquid-network problems and it is thus shown to be well-behaved, reliable and stable throughout execution. The importance of this feature cannot be overstated as the popular and widespread application of Newton-Raphson-based protocols requires initial guesses for the first iteration. Once a nodal pressure solution is available, decompression ratios and linear-analog conductivities are updated. Successive iterations will follow until calculated nodal pressures do not significantly change within a prescribed tolerance. Actual C_{ij} values are also updated at each iteration, using the appropriate friction factor functional form in **Table 3.1** that corresponds to the gas flow equation being implemented. Besides, the proposed linear-analog method also does not require the formulation of loop equations, and solely relies on nodal connectivity information, contrary to other network methods such as the loop and loop-nodal formulations. The advantages and disadvantages of the linear-analog method are summarized at **Table 6.1** below. As demonstrated, linear-analog iterations are

inexpensive in both implementation and execution when compared to Newton-Raphson iterations because they do not rely on Jacobian or derivative calculations.

Essentially, the linear-analog method presented is able to solve gas load flow problems for any fluid system without the need for heavy computational power. The method successfully preserves all the advantages of the Newton-nodal method while truncating the need for initial guesses and, at the same time, it also eliminates the needs for Jacobian formulations and calculation of derivatives. However, a potential drawback of the proposed method is that its convergence is non-quadratic and more analog iterations may be required for final convergence once the iterative solution gets close to the actual solution. For iterative solutions that are close to the actual solution, Newton-Raphson protocols could become more efficient once initialized using linear-analog-generated initial values. A hybrid approach can be devised where the linear-analog method is first implemented to inexpensively and reliably advance the network solution up to a point where the quadratic convergence of the nodal Newton-Raphson protocol can be fully taken advantage of without diverging hopelessly.

Subsequently, a wider range of pipeline network system analyses could then be executed with ease. One of the most important applications of pipe network analysis, such as the one applied to the system in **Figure 1.1,** is its ability to carry out network-wide sensitivity analysis. Sensitivity analysis is used to prioritize what changes in network components are the most important for the improvement of overall network performance. This can be

especially critical when the demands or supplies in the system change in time and network adjustments are required. The quantification of how sensible flow variables are to changes in one variable or several design variables can provide a much deeper understanding of network performance. This analysis typically leads to the identification of the network component whose adjustment or replacement is most likely to help overcome deficiencies in any network performance.

Table 6.1: Summary of Linear-Pressure Analog Method vs. Newton-Raphson Nodal Method

Linear-Pressure Analog Method	**Newton-Raphson Nodal Method**
No initial guesses needed	Initial guesses needed to initiate Newton-Raphson iterative protocol
Stable convergence behavior	Convergence severely dependent on user-defined initial guesses
Inexpensive and straightforward solution of linear system of simultaneous equations	Potentially expensive Jacobian matrix calculations
Non-quadratic convergence	Convergence highly dependent on initialization; quadratic once close to the solution.
No need for loop information	No need for loop information

BIBLIOGRAPHY

Ayala, L. F. (2012). Chapter 21: Transportation of Crude Oil, Natural Gas, and Petroleum Products. *ASTM Handbook of Petroleum and Natural Gas Refining and Processing*. ASTM International.

Boyd, O. W. (1983). *Petroleum Fluid Systems.* Norman: Campbell Petroleum Series.

Brebbia, C. A., and Ferrante, A. J. (1983). Computational Hydraulics. Butterworth-Heinemann Ltd.

Crafton, J. W. (1976, October 3-6). An Iterative Solution for the Gas Pipeline Network Problem. *SPE 6032*. Dallas, Texas, United States of America: Society of Petroleum Engineers Journal.

Cross, H. (1932). Analysis of Continuous Frames by Distributing Fixed-End Moments. *Transactions of ASCE, v 96, n 1793*, 1-10.

Dranchuk, P. M., and Abou-Kassem, J. H. (1975). Calculation of Z Factors For Natural Gases Using Equations of State. *Journal of Canadian Petroleum Technology*, 34-36.

Golan, M., and Whitson, C. H. (1991). *Well Performance.* Englewood Cliffs: Prentice Hall.

Ikoku, C. U. (1984). *Natural Gas Production Engineering.* New York: John Wiley and Sons.

Johnson, T. W., and Berwald, W. B. (1935). *Flow of Natural Gas Through High-Pressure Transmission Lines.* U.S. Department of the Interior Bureau of Mines.

Larock, B. E., Jeppson, R. W., and Watters, G. Z. (1999). *Hydraulics of Pipeline Systems.* CRC Press.

Li, Q., An, S., and Gedra, T. W. (2003). Solving Natural Gas Loadflow Problems Using Electric Loadflow Techniques. Stillwater.

Mageid, H. A., Hago, A. W., and Magid, I. A. (1991). Analysis of Pipe Networks by the Finite Element Method. *Water International*, Vol. 16, Iss. 2.

Martinez-Romero, N., Osorio-P, O., and Santamaria-V., I. (2002). Natural Gas Network Optimization and Sensibility Analysis. *SPE Paper 74384*. Society of Petroleum Engineers.

Menon, E. (2005). *Gas Pipeline Hydraulics.* Boca Raton: CRC Press Taylor and Francis Group.

Mohitpour, M., Golshan, H., and Murray, A. (2007). *Pipeline Design and Construction.* New York: ASME Press.

Montoya-O., S. J., Jovel-T., W. A., Hernandez-R, J. A., and Gonzalez-R, C. (2000). Genetic Algorithms Applied to the Optimum Design of Gas Transmission Networks. *SPE 59030*. Society of Petroleum Engineers.

Murphy, H. G. (1989, October 19-20). Compressor Performance Modeling to Improve Efficiency and the Quality of The Optimization Decisions. *PSIG*. El Paso, Texas, United States of America: Pipeline Simulation Interest Group.

Nagoo, A. S. (2003, August). Analysis of Steady and Quasi-Steady Gas Flows in Complex Pipe Network Topology. PA, United States of America: The Pennsylvania State University Graduate School.

Osiadacz, A. J. (1987). *Simulation And Analysis of Gas Networks.* Houston: Gulf Publishing Company.

Press, W. H., Teukolsky, S. A., Vetterling, W. T., and Flannery, B. P. (2002). *Numerical Recipes in C++: The Art of Scientific Computing Second Edition.* New York: Cambridge University Press.

Rawlins, E. L., and Schellhardt, M. A. (1936). Back-Pressure Data on Natural Gas Wells and Their Application to Production Practices. U.S. Bureau of Mines Monograph 7.

Schroeder, D. W. (2011, August 16). A Tutorial on Pipe Flow Equations. Carlisle, Pennsylvania: Stoner Associates, Inc.

Sutton, R. P. (1985). Compressibility Factors for High-Molecular-Weight Reservoir Gases. *SPE 14265*. Las Vegas, Nevada, USA: SPE.

Weymouth, T. R. (1912). Problems in Natural Gas Engineering. *Transactions of ASME v. 34*, 185-206.

Wood, D., and Carl, O.A , Hydraulic Network Analysis Using Linear Theory, *Journal of the Hydraulics Division, ASCE,* vol. 98, No. 7, July, pp. 1157-1170, 1972.

Zhou, J., and Adewumi, M. A. (1998, November 9-11). Gas Pipeline Network Analysis Using an Analytical Steady-State Flow Equation. *SPE 51044*. Pittsburgh, PA, United States of America: Society of Petroleum Engineers.

APPENDIX

The model in this thesis was developed using two separate programs. The input data will be read and manipulated on an Excel Spreadsheet. Users will have to have Microsoft Excel installed on their computer platforms. On the other hand, the algorithm for the model is done in MATLAB by MathWorks. The Appendix will explain the algorithm behind the codes and how users could implement that for each case study presented here.

A1 – Input Data for Case Study

GasNet v1.0 by Chew Y. Leong	
Solution Method	1
Pipe Equation	5
Gas Properties	
Average Temperature (R)	535
Specific Gravity	0.69
Compressibility Factor	0.9

Solution Method [1, 2] is where users select 1 for solving the system with Linear Analog Method or 2 for solving with Newton-Raphson procedure.

Pipe Equation [1, 2, 3, 4, 5] is where users select 1 for Generalized Flow Equation, 2 for Weymouth friction Factor, 3 for Pandhandle-A, 4 for Panhandle-B and 5 for Fully Turbulent AGA.

The program requires the users to input the gas properties where:

Average Temperature [Value] is where users input the average gas temperature in Rankine.

Specific Gravity [Value] is where users input the specific gravity of gas.

Compressibility Factor [Value] is where users input the average gas compressibility factor. If gas compressibility factor is deemed not to be average, the users will input 0 for gas compressibility calculation based on (Dranchuk and Abou-Kassem, 1975).

Total No. of Pipes	12	Pipes										
Pipe	1	2	3	4	5	6	7	8	9	10	11	12
Up Node	1	2	1	2	3	4	5	4	5	6	7	8
Down Node	2	3	4	5	6	5	6	7	8	9	8	9
Diameter (in)	6.065	6.065	6.065	4.026	4.026	4.026	4.026	6.025	4.026	4.026	4.026	4.026
Length (Miles)	30	30	30	30	30	30	30	30	30	30	30	30
Change in Height (ft)	0	0	0	0	0	0	0	0	0	0	0	0
Roughness	0.0018	0.0018	0.0018	0.0018	0.0018	0.0018	0.0018	0.0018	0.0018	0.0018	0.0018	0.0018
Check Valve	0	0	0	0	0	0	0	0	0	0	0	0
Pipe Efficiency	1	1	1	1	1	1	1	1	1	1	1	1

Total No. of Pipes [Value] is where users input the total number of pipes in the system. Users then click on the *Pipes* button to generate the number of columns based on the input.

Pipe is automatically generated.

Up Node [Value] is where users input the upstream node of the pipe. It could be a guess if the node is not known before since the program will correct it as it iterates through the solution.

Down Node [Value] is where users input the downstream node of the pipe. Again, users could just guess it if the node is not known.

Diameter [Value] is where users input the diameter of each pipe segment in inches.

Length [Value] is where users input the length of each pipe segment in miles.

Change in Height [Value] is where users input the elevation in term of feets for each pipe segment measured from the base datum.

Roughness [Value] is where users input the roughness factor of the pipe segment.

Check Valve [1, 0] is where users select 1 if check valve is installed on pipe to avoid backflow and 0 if there is no check valve installed.

Pipe Efficiency [Value] is where the users input the efficiency of the pipe for calibration purposes.

Total No. of Nodes	9	Nodes							
Node	1	2	3	4	5	6	7	8	9
Supply [-] /Demand [+] (MMSCFD)	-16	2	2	3	1	2	2	2	2
Initial Pressure Guess									

Total No. of Nodes [Value] is where users input the total number of nodes in the system. Users then press *Nodes* button to generate the specified number of nodes.

Node is automatically generated.

Supply [-] / Demand [+] [Value] is where users input the supply and demand of each node in terms of MMSCFD.

Initial Pressure Guess is only applicable when users select Newton-Raphson procedure for solving the system.

Total No. of Specified Nodes	1	Sp. Nodes
Node with Specified Pressure	9	
Specified Pressure (Psia)	130	

Total No. of Specified Nodes [Value] is where users input the total number of specified nodes in the system. Users then click on *Sp. Nodes* button to generate the columns according to the total number.

Node with Specified Pressure [Value] is where users input the location of the specified nodes. *Caution: users want to make sure that whenever possible the node with lowest pressure should be specified to avoid overestimating the lowest pressure. Users should also specify exit nodes when there are wells since the total demand of the system is unknown.*

Total No. of Wellheads	0	Wells
Node as Wells		
Well Conductivity (MMSCFD/psia)		
Shut-In Pressure (Psia)		
Flow Exponent		

Total No. of Wellheads [Value] is where users input the total number of wellheads of the system. Users should then click *Wells* button to generate the columns needed for data input.

Node as Wells [Value] is where users input the location of the well according to the nodes.

Well Conductivity [Value] is where users input the data for C_w for each well in units of (MMSCFD/psia)

Shut-In Pressure [Value] is where users input the data for the shut-in pressure of the well in terms of Psia.

Flow Exponent [0.5-1] is where users input the data for the flow exponent of the particular well.

Total No. of Compressors	0	Compressors
Compressors		
Up Node		
Down Node		
Specific Heats of Gas [γ]		
Adiabatic Efficiency		
Suction Temperature (R)		
Compressor Ratio Specified		
Horsepower Specified (HP)		

Total No. of Compressors [Value] is where users input the data for the total number of compressors in the system. Users then click on *Compressors* button to generate the number of columns according to the total number.

Compressors are automatically generated.

Up Node [Value] is where users input the upstream node of the compressor.

Down Node [Value] is where users input the downstream node of the compressor.

Specific Heats of Gas [Value] is where users input the specific heats of gas or polytropic exponent in polytropic process.

Adiabatic Efficiency [Value] is where users input the value of the efficiency of the compressor.

Suction Temperature [Value] is where users input the value of the suction temperature for the gas in Rankine.

Compressor Ratio Specified [Value] is where users input the value of compression ratio for the compressor. It is only applicable if the users are selecting Linear-Analog method as the model.

Horsepower Specified [Value] is where users input the value of horsepower of the compressor in terms of HP. It is only applicable if the users are selecting Newton-Raphson method for the solution model.

A2 – Linear-Analog Algorithm

The implementation of the linear-analog method relies fundamentally on the way users define their system since network could be expressed in incidence matrix. The code snippets below show how the matrix could be formed. The program below is written in MATLAB coding language.

```
 %Initializing matrix
   matrix=zeros(nodes_no);
    residual=zeros(nodes_no,1);

%Forming upper and lower matrix
for ii=1:pipes_no

matrix(up_node(ii),dn_node(ii))=C(ii);
matrix(dn_node(ii),up_node(ii))=C(ii);
   if abs(s(ii))>0
      matrix(up_node(ii),dn_node(ii))=exp(s(ii)/2)*matrix(up_node(ii),dn_node(ii));
   end
end

%Including Compressors
if comp_no~=0
   for ii=1:comp_no
      matrix(comp_upnode(ii),comp_dnnode(ii))=-Cc(ii);
      for jj=1:pipes_no
         if up_node(jj)==comp_dnnode(ii)
            matrix(comp_dnnode(ii),comp_upnode(ii))=-compratio(ii)*C(jj);
            matrix(dn_node(jj),up_node(jj))=0;
            matrix(dn_node(jj),comp_upnode(ii))=compratio(ii)*C(jj);
         end
      end
   end
end
```

In order to form the characteristic matrix **K**, the upper and lower matrixes are first formed with the codes above. It then checks if compressor is included in the system and compressors constants are included in the characteristic matrix **K.**

```
    %Forming Diagonal Entries
    %Forming Residual Vector
column=1;

    %Including Pipes
    for row=1:nodes_no
          for loop=1:pipes_no
             if up_node(loop)==row
                 matrix(row,column)=-C(loop)+matrix(row,column);
             end

             if abs(s(loop))>0 andand dn_node(loop)==row
                 matrix(row,column)=-exp(s(loop)/2)*(C(loop))+matrix(row,column);
             elseif dn_node(loop)==row
                 matrix(row,column)=-C(loop)+matrix(row,column);
             end

          end
    residual(row)=supply_demand(row)*10^6+residual(row);

    %Including Wells
     if wells_no~=0
          for loop=1:wells_no
             if row==wells(loop)
             matrix(row,column)=-wellc(loop)+matrix(row,column);
             residual(wells(loop))=-wellc(loop)*Pshut(loop)+residual(wells(loop));
             end
          end
     end

    %Including Compressors
       if comp_no~=0
          for cloop=1:comp_no
           if comp_dnnode(cloop)==row
              matrix(row,column)=Cc(cloop);
           end
          end
       end
```

The diagonal entries, O_i and the residual vector or the network consumption/demand vector, **P** are then formulated according to the algorithm listed above.

```
        %Including Specified Nodes
       for i=1:spnodes_no
          if row==nsp(i)
             matrix(row,:)=0;
             matrix(row,column)=1;
          end
       end
          column=column+1;

end
%Including Specified Nodes in Residual
       for i=1:spnodes_no
           residual(nsp(i))=sp_pressure(i);
       end

    %Shutting Node to prevent backflow if check valve is installed
     for i=1:nodes_no
        if off(i)==1
           residual(i)=pressure(dn_node(i));
           matrix(i,i)=1;
        end
     end

     %Calculating New Pressures
           pressure_old=pressure;
           pressure=matrix\residual;

     %Calculate HP
      if comp_no~=0
        for i=1:comp_no
           HP(i)=pressure(comp_dnnode(i));
           pressure(comp_dnnode(i))=compratio(i)*pressure(comp_upnode(i));
        end

      end
```

Nodes with specified pressures are then substituted in the network consumption/demand vector, **P** and if there is compressor, the pressure is updated with the compression ratio and calculated upstream node pressure.